

LOOK BEFORE YOU LEAP: UNIVERSAL EMERGENT MECHANISM FOR RETRIEVAL IN LANGUAGE MODELS

Alexandre Variengien*
EU AI Office
European Commission

Eric Winsor*
UK AI Security Institute

ABSTRACT

When solving challenging problems, language models (LMs) are able to identify relevant information from long and complicated contexts. To study how LMs solve retrieval tasks in diverse situations, we introduce ORION, a collection of structured retrieval tasks, from text understanding to coding. We apply causal analysis on ORION for 18 open-source language models with sizes ranging from 125 million to 70 billion parameters. We find that LMs internally decompose retrieval tasks in a modular way: middle layers at the last token position process the request, while late layers retrieve the correct entity from the context. Building on our high-level understanding, we demonstrate a proof of concept application for scalable internal oversight of LMs to mitigate prompt-injection while requiring human supervision on only a single input.

1 INTRODUCTION

Recent advances in language models (LMs) (Vaswani et al., 2017) have demonstrated their flexible problem-solving abilities and their expert-level knowledge in a wide range of fields (Bubeck et al., 2023; OpenAI, 2023). Researchers have developed a series of techniques such as fine-tuning (Ouyang et al., 2022) and Reinforcement Learning from Human Feedback (RLHF) (Ouyang et al., 2022) to ensure models output honest and helpful answers. However, as their abilities reach human level, supervision from human feedback becomes costly and even impossible. This necessitates more efficient or automated methods of supervision, known generally as *scalable oversight*.

Moreover, existing methods only control for the output of the model while leaving the internals of the model unexamined (Casper et al., 2023; Ngo et al., 2023). This is a critical limitation as many internal processes can elicit the same output while using trustworthy or untrustworthy mechanisms. For instance, we would like to know whether a model answers faithfully based on available information or simply gives a user’s preferred answer (Perez et al., 2022). We call this problem *internal oversight*.

Recent works on mechanistically interpreting LMs have shown success on narrow tasks (Wang et al., 2022; Nanda et al., 2023). Some have provided insight into factual recall (Geva et al., 2023) and in-context learning (Olsson et al., 2022). Causal interventions have even been used to understand how models encode tasks from few shot examples (Hendel et al., 2023) or bind entities to attributes (Feng and Steinhardt, 2023). However, these works are still scoped to relatively narrow contexts and lack demonstration of concrete applications.

In this work, we study how LMs solve retrieval tasks, i.e. in-context learning problems that involve answering a request (e.g. “What is the city of the story?”) to retrieve a keyword (e.g. “Paris”) from a context (e.g. a story).

We start by introducing ORION, a collection of 15 datasets of retrieval tasks spanning six different domains from question answering to coding abilities and variable binding. We systematize the task structure by annotating each textual input with an abstract representation where the context is a table of attributes, and the request is a simple SQL-like query, as illustrated in Figure 2.

We apply causal analysis (Pearl, 2009; Vig et al., 2020; Geiger et al., 2021) to 18 open source LMs ranging in size from 125 million to 70 billion parameters to investigate the successive role of layers

*Work conducted while at Conjecture. Corresponding author: alexandre.variengien@gmail.com

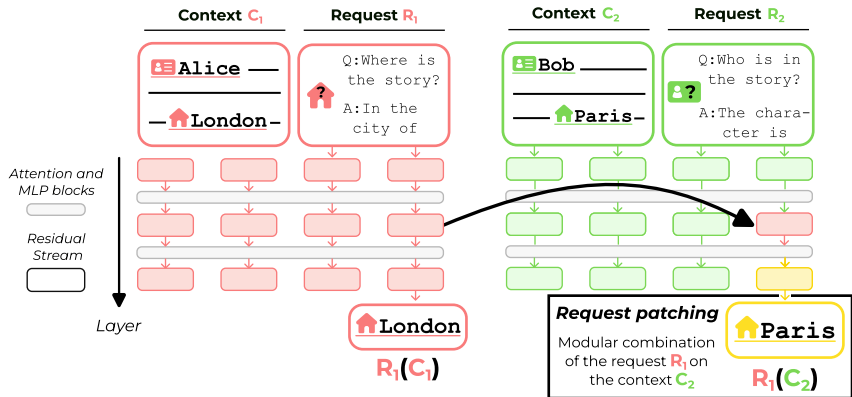


Figure 1: Illustration of our main experimental discovery. Patching the mid-layer residual stream on a retrieval task from ORION causes the language model to output a modular combination of the request from x_1 (asking for the city) and the context from x_2 (a story about Bob in Paris). We call this phenomenon *request-patching*.

at the last position on tasks from ORION. The shared abstract representation enables us to define and interpret experiments across tasks and models at scale, without the need for setting-specific labor. We discover that language models handle retrieval tasks by cleanly separating the layers at which they process the request and the context at the last token position. These results suggest that there exists an emergent modular decomposition of tasks that applies across models and tasks. We complement this coarse-grained causal analysis with a finer-grained case study of a question-answering task on Pythia-2.8b (Biderman et al., 2023).

We demonstrate that our understanding of how models solve retrieval tasks can be directly leveraged to mitigate the effect of prompt injection (Perez and Ribeiro, 2022) in a question-answering task. Models are given inputs containing distractor sequences that trigger models to output a token unrelated to the task. We present a proof-of-concept based on request-patching that only requires humans to verify the model output on a *single* trusted input. Our technique significantly improves the performance of models on sequences with distractors (0% \rightarrow 70.5% accuracy for Pythia-410m, 15.5% \rightarrow 97.5% for Pythia-12b). To our knowledge, this is the first demonstration that scalable internal oversight of LMs is feasible.

In summary, our main contributions are as follows:

1. We introduce ORION, a collection of structured retrieval tasks. It is a data-centric approach enabling a comparative study of 18 models on 6 domains.
2. We discover a macroscopic modular decomposition of retrieval tasks in LMs’ internals that is universal across tasks and models.
3. We link macroscopic and microscopic descriptions of LMs’ internals with a fine-grained case study of a question-answering task on Pythia-2.8b.
4. We apply this knowledge to a proof of concept for *scalable internal oversight* of LMs solving a retrieval task in the presence of prompt injection.

2 BACKGROUND

2.1 THE TRANSFORMER ARCHITECTURE FOR AUTOREGRESSIVE LANGUAGE MODELS

An autoregressive language model, \mathcal{M}_θ with parameters θ , maps a sequence of input tokens $x = (x_1, x_2, \dots, x_n)$ to a probability distribution over the next token x_{n+1} . For the Transformer architecture (Vaswani et al., 2017), we have:

$$\begin{aligned}
 p(x_{n+1}|x) &= \mathcal{M}_\theta(x) \\
 &= \text{softmax}(\pi_n(x))
 \end{aligned}$$

The pre-softmax values π_n are the logits at the n -th token position. The final logits π_l are constructed by iteratively building a series of intermediate activations z_k^l we call the *residual stream*, following Elhage et al. (2021). The residual stream z_k^l at token position k and layer l is computed from the residual stream at previous token positions at the previous layer $z_{\leq k}^{l-1}$ by adding the results of a_k^l , a multi-headed attention module that depends on $z_{\leq k}^{l-1}$, and m_k^l , a two-layer perceptron module that depends on z_k^{l-1} . We provide a complete description of the Transformer architecture in Appendix G.

2.2 COMPUTATIONAL GRAPH AS CAUSAL GRAPH

The experimental paradigm of causal analysis applied to machine learning models initiated by (Vig et al., 2020) and (Geiger et al., 2021) treats the computational graph of a neural network as a causal graph. The goal of causal analysis is to answer questions about *why* a model outputs a given answer. This requires uncovering the causal links tying the inputs to the output, as well as characterizing the role of the internal components critical for the model’s function. To this end, researchers rely on *causal interventions* (Pearl, 2009), experiments that replace a set of activations with fixed values.

In this work, we use single-input *interchange intervention*¹ (Geiger et al., 2021). It is a simple form of causal intervention where we intervene on one variable at a time by fixing its value to be the value of that same variable on another input. We write $\mathcal{M}(x|A \leftarrow A(x'))$ the output of the model after the single-input interchange intervention on the *target input* x , replacing the activation of the node A by its value on the *source input* x' .

3 ORION: A COLLECTION OF STRUCTURED RETRIEVAL TASKS

Our study concentrates on retrieval, a fundamental aspect of in-context learning, which involves answering a request (e.g. “What is the name of the city?”) by identifying the correct attribute (e.g. a city name) from the context (e.g. a story). To facilitate this study, we crafted a collection of datasets dubbed the **Organized Retrieval Operations for Neural networks (ORION)**.

Abstract representation. Each textual input (i.e. LM prompt) from ORION is annotated with an abstract representation (C, R) where C represents the context and R the request. In the example of Figure 2, the context is a story introducing a place, a character, and an action, while the request is a question written in English asking for the city of the story.

The context C is abstractly represented as a table where each line is a list of attributes. The request R is retrieving a target attribute $ATTR_t$ (e.g. the “name” attribute in Figure 2), from lines where a filter attribute $ATTR_f$ (e.g. the narrative role) has the value v_f (e.g. “city”). The request can be written using a language in the style of SQL as follows: `SELECT $ATTR_t$ FROM C WHERE $ATTR_f = v_f$` (e.g. `SELECT Name FROM Context WHERE Role=City`).

We note $R(C)$ the results of applying the request on the context. This is the ground truth completion for LMs evaluated on the retrieval task. In practice, $R(C)$ is a single token called the *label token*. On the example we have $R(C) = \text{“ Valencia”}$.

Desiderata for datasets. To facilitate the application of causal analysis, we enforce a list of desiderata on datasets from ORION. The most important desiderata is ensuring datasets are *decomposable*. For every dataset D in ORION, for every abstract representations $(C_1, R_1), (C_2, R_2)$ in D , $R_2(C_1)$ and $R_1(C_2)$ are well-defined. This means that an arbitrary request can be applied to an arbitrary context from the same task. Abstract representations of requests and contexts can be freely interchanged across a task. This constraint enables the design of interchange interventions at scale.

We define four additional desiderata Structured, Single token, Monotasking, and Flexible in Appendix H and share the motivation behind their definition.

Dataset composition. The dataset includes the retrieval task from domains: question-answering, translation, factual recall, variable binding, induction pattern-matching, and type hint understanding. For each domain, we created two or three variations. Each dataset is created using a semi-automated process leveraging the LLM assistant ChatGPT. We provide a detailed overview of the dataset and its creation in Appendix H.

¹It is sometimes called “activation patching” in the literature see e.g. Wang et al. (2022)

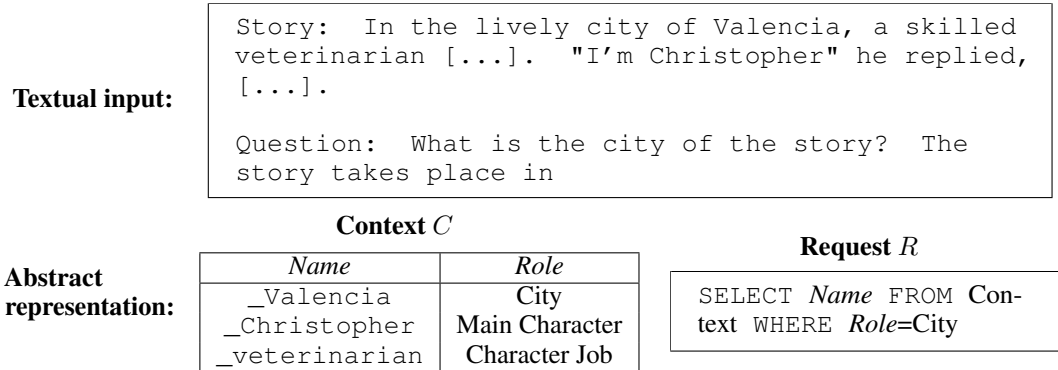


Figure 2: Example input from ORION for the question-answering task. Textual inputs are annotated with an abstract representation of the context and the request. Abstract context representations are tables where each line lists attributes relative to a story element. Requests can be formulated using simple SQL-like queries.

Performance metrics. We define a task T as a set of input-output pairs (x, y) where x is the LM input and y is the expected label token. We use two main metrics to quantify the performance of a language model on an ORION task T .

- **Accuracy:** $\mathbf{E}_{(x,y) \sim T}[\mathcal{M}(x) = y]$
- **Token probability:** $\mathbf{E}_{(x,y) \sim T}[p(y|x)]$

Accuracy serves as our primary metric to assess model performance in solving tasks due to its straightforward interpretation and practical application in language models, where the most probable token is often chosen.

However, accuracy falls short in capturing nuanced aspects of predictions, for instance, accuracy doesn't measure the margin by which a token is the most probable. To have a granular evaluation of model behavior after interventions, we employ token probability, offering a continuous measure.

We evaluate the performance of 18 models from four different model families: GPT-2 (Radford et al., 2019), Pythia (Biderman et al., 2023), Falcon (Almazrouei et al., 2023) and Llama 2 (Touvron et al., 2023). We study base language models for all families except Falcon where we include two instruction fine-tuned models. We choose the models to capture diverse scales, architecture, and training techniques.

Unsurprisingly, larger models can solve a wider range of problems. Models with more than 6 billion parameters are able to solve every task with more than 70% accuracy. Nonetheless, even GPT-2 small with 125M parameters, one of the smallest models, can solve the simplest version of the question-answering task with 100% accuracy. Detailed evaluations using the token probability and logit difference are available in Appendix A.

In the following analyses, we only consider settings where the model can robustly solve the task. Thus, we focus on pairs of models and tasks that have greater than 70% accuracy.

4 MACROSCOPIC CAUSAL ANALYSIS ON ORION: A UNIVERSAL EMERGENT DECOMPOSITION OF RETRIEVAL TASKS

To correctly solve retrieval tasks, an LM has to gather and combine at the last token position information coming from the request and the context. We focus our investigations on understanding how these two processing steps are organized in the intermediate layers of the last token position.

In this section, we choose to consider a coarse-grained division of the model, intervening on full layers instead of a finer-grained division, e.g. considering single-attention heads and MLP blocks. We find this level of analysis is sufficient to develop a high-level causal understanding of how language models solve retrieval tasks while providing a computationally tractable set of experiments to run at



Figure 3: Normalized token probability and accuracy for the label tokens $R_1(C_1)$, $R_1(C_2)$ and $R_2(C_2)$ after patching the residual stream across all layers. Patching early (before $L_1 = 13$) and late (after $L_3 = 27$) leads to the expected results, respectively no change in output and patching the output from x_1 . However, intervening on the middle layer ($L_2 = 16$) leads to the model confidently outputting the token $R_1(C_2)$, a modular combination of the request from x_1 and the context from x_2 .

scale. We complement this general coarse-grained analysis in Section 5 with a finer-grained case study on Pythia-2.8b solving a question-answering task.

4.1 METHODS

Our main experimental technique is *residual stream patching*. Residual stream patching is a single-input interchange intervention, replacing the residual stream at a layer L at the last position in the forward pass of the model on input x_2 with its activation from another input x_1 . Following the notation introduced in Section 2.2, we note $\mathcal{M}(x_2|z_n^L \leftarrow z_n^L(x_1))$ the model output on x_2 after this intervention.

As shown in Figure 1, residual stream patching makes every component before layer L have the activation it takes on x_1 while the components after layer L receive mixed activations (denoted by the yellow color in the figure). These later layers see activations at the last position coming from x_1 while activations from earlier positions come from x_2 .

To characterize the output of the patched model, we measure the token probability and accuracy for three different label tokens related to the inputs x_1 and x_2 . We use both label tokens from the input x_1 and x_2 , $R_1(C_1)$ and $R_2(C_2)$ respectively, and the label token $R_1(C_2)$ that is the result of applying the request from x_1 on the context of x_2 .

To facilitate comparisons between different tasks and models, we normalize the token probability based on the mean probability of the correct token given by the model for the task. In addition, we calculate the normalized accuracy where 0 represents the accuracy of random guess, i.e. responding to a random request in a given context while 1 denotes the model’s baseline accuracy for that task.

We perform residual stream patching at the last position for every layer, model, and task of ORION. For each task, we use a dataset of 100 prompts and average the results of 100 residual stream patching experiments with x_1 and x_2 chosen uniformly from the task dataset.

4.2 RESULTS OF RESIDUAL STREAM PATCHING

Figure 3 shows the results of residual stream patching on the question-answering task with a uniform answer prefix for the Pythia-2.8b model. We observe that after residual stream patching on the layer before layer 13, the model is outputting $R_2(C_2)$ with 100% normalized token probability. Our interpretation is that this intervention does not perturb the model processing of x_2 . We further observe that residual stream patching after layer 27 causes the model to output $R_1(C_1)$ with more than 80% normalized token probability. In effect, patching the residual stream after a certain layer is equivalent to hard-coding the model output on x_1 .

Surprisingly, when patching between layers 15 and 16, we observe that the model outputs $R_1(C_2)$ with 100% normalized accuracy, i.e. with the same accuracy level as the baseline task accuracy. The model is outputting the results of the request contained in the input x_1 in the context of the input x_2 .

We call this phenomenon, *request-patching*, i.e. a residual stream patching experiment that leads to the $R_1(C_2)$ label token being confidently outputted by the patched model. Such results demonstrate that the causal intervention coherently intervenes in the model’s internal computation, causing it to modularly combine high-level information from two different prompts.

We observe a sudden jump in the normalized accuracy of request-patching from 0 to 1 between layers 14 and 15. However, it is likely that transforming the sequence of tokens representing the question into a representation of the request takes several layers. Thus, we hypothesize that a large part of the request processing happens at the previous token positions of the question. In this interpretation, the observed jump at layer 15 results from the intermediate representation of the request being propagated to the last position through attention modules.

Defining limit layers. From the results of the residual stream experiments, we define three layers – L_1 , L_2 , and L_3 – delimiting the three different outcomes of residual stream patching as shown in Figure 3.

L_1 is the maximal layer at which the normalized token probability of the label token $R_1(C_1)$ is greater than 80%. It marks the end of the region where residual stream patching does not interfere with the model output. L_2 is the layer where the normalized probability of the label $R_1(C_2)$ is maximal. It is the place where the effect of request-patching is the strongest. L_3 is the minimal layer where the normalized probability of the label $R_2(C_2)$ is greater than 80%. It marks the start of the region where residual stream patching leads to a complete overwrite of the model output.

We choose the token probability as a continuous metric to measure the model prediction. The 80% threshold has been chosen arbitrarily as a criterion to consider that the model is mainly outputting a single label token.

Request-patching is general across models and datasets. We expand our investigation of request-patching to include every model and task from ORION. To ease the analysis, we compute the maximal normalized probability of the $R_1(C_2)$ label token, i.e. the normalized probability after patching at L_2 . We use this metric as our main performance indicator to measure the strength of the request-patching phenomenon on a given pair of model and task.

98 out of the 106 pairs of tasks and models studied demonstrate a similar profile as the one shown in Figure 3. Request-patching leads to at least 70% normalized probability of the $R_1(C_2)$ label token. Request-patching appears across variations in domain, task complexity, and low-level prompt structure. Moreover, it is present in every model studied, from GPT-2 small to Llama 2 70b, one of the largest available open-source LMs.

The results for the question-answering with mixed template task demonstrate that request-patching works even when patching the residual stream across different templates, e.g. taking the residual stream from a prompt where the question is *before* the story and patching it in a model execution where the question is *after* the story. This means that the representation stored in the patched activation is related to the semantic meaning of the question, and not surface-level textual features.

However, the phenomenon of request-patching seems not to be present in the abstract induction task on large models. We hypothesize that this is due to the increased wideness of large models and the simplicity of the task. We discuss further the results for induction and factual recall by comparing request-patching results to prior work in Appendix F.

To further our analysis, Figure 4 shows the values of the layer L_2 on different models and datasets. We observe that the effect of request-patching for the induction tasks is the strongest at earlier layers compared to the other tasks. This observation is consistent with the simplicity of the request processing, which only involves copying previous tokens. The L_2 layers for other tasks are concentrated in similar layers, suggesting a similar high-level organization of the internal computation that does not depend on the details of the task being solved. However, for Llama 2 70b, the largest model studied, the L_2 layers are concentrated in the same narrow range (39-43) for every task, including the simple induction tasks. It is unclear if this disparity is caused by its larger size or by the specifics of the architecture. We provide visualizations of request patching results and of layers L_1 and L_3 in Appendix D.

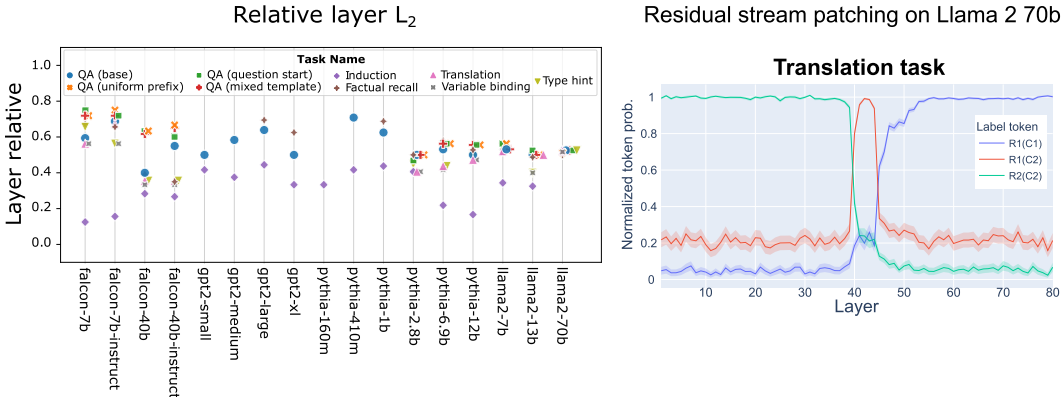


Figure 4: **Left:** Layer of maximal request-patching performance L_2 for different models and tasks. While the L_2 layers for most tasks are concentrated at similar layers, the processing of the request in the induction task seems to happen at earlier layers. **Right:** results of residual stream patching on Llama 2 70b. Request-patching is most performant in a narrow range of layers centered around layer 42 and does not depend on the nature of the task.

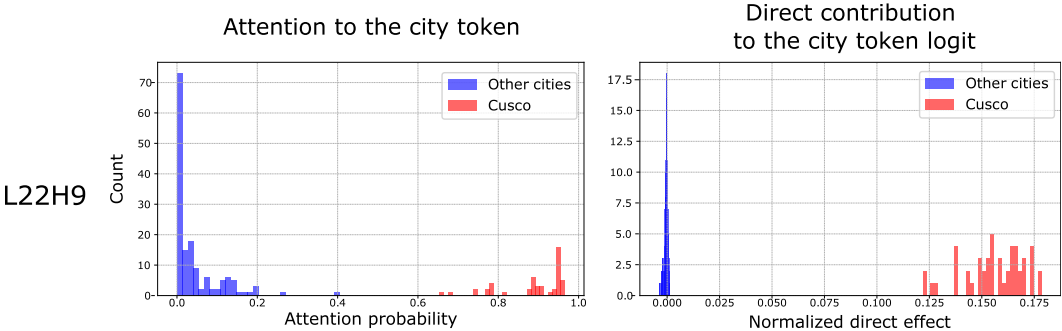


Figure 5: City-specific heads attend to the city token and contribute directly to the logits when the question asks about the city of the story *only* if the city has a specific value, e.g. “Cusco”.

5 MICROSCOPIC ANALYSIS: CASE STUDY ON PYTHIA-2.8B

To complement the high-level causal explanation described in the previous section, we conduct a finer-grained case study on Pythia-2.8b on the question-answering task. Our motivation is twofold. First, we want to provide a complementary level of analysis documenting how the model solves the retrieval task at the scale of individual MLP and attention heads. Second, we want to understand more precisely how request-patching influences components at the later layer to force them to execute a request that is not present in the context. Appendix B describes in detail our methodology and the results of the case study. In this section, we provide an overview of our key results.

The components contributing directly to the logits depend on superficial changes in the input. We discover that the set of components directly influencing the logits varies from input to input. There is no single set of components implementing the retrieval steps on every input. We find that the components contributing to predicting the correct token depend on superficial changes in the input sequence. As shown in Figure 5, we discover a family of attention heads that retrieve the correct token from the context when the question asks for the city of the story *only* when the city has a particular value (e.g. “Cusco”). For all the other city names, these heads do not directly contribute significantly to the output.

Request-patching preserves natural mechanism. To compare the internal changes caused by residual stream patching $\mathcal{M}(x_2|z_n^{L_2} \leftarrow z_n^{L_2}(x_1))$ to a natural mechanism, we construct a reference input x_3 by concatenating the textual representation of the context C_2 and the request R_1 . On x_3 ,

the model is naturally executing the request R_1 on the context C_2 . This reference input acts as our control condition to compare the effect of request-patching.

We find that request-patching globally preserves the mechanism of the components at the late layers. We measure the direct effect and attention pattern for every component after patching $\mathcal{M}(x_2|z_n^{L_2} \leftarrow z_n^{L_2}(x_1))$. These measures are similar to those of the components on the corresponding reference input x_3 (relative difference less than 12%). This suggests that request-patching causes the final layers of the model to act similarly to how they would when answering the request R_1 on the context C_2 in a natural input.

Microscopic vs Macroscopic analysis. The clear division between the request processing and retrieval step observed at a macroscopic level does not translate into a similar level of modularity at a microscopic level. Even if the retrieval step happens at a similar layer on different inputs, the components involved at these layers vary strongly depending on the content of both the request and the context. Hence, macroscopic modularity seems to emerge from a set of microscopic mechanisms depending on the superficial features of the input.

Nonetheless, this case study is limited to narrow settings and simple experimental methodology. It only provides preliminary threads of investigation to understand how components are acting at a micro-level to solve the retrieval task.

6 APPLICATION TO SCALABLE INTERNAL OVERSIGHT OF A RETRIEVAL TASK

Model	Intervention	No distractor	Small-model distractor	Large-model distractor	Control distractor
Pythia-410m	No intervention	97	0	84	100
	Request-patching	100	70.5	100	100
Pythia-12b	No intervention	100	90.5	15.5	100
	Request-patching	98	89.5	97.5	98.5

Table 1: Accuracy (in %) on the question-answering task before and after request-patching from a trusted input. Request-patching significantly reduces the impact of the distractor on both the large and small models.

Language models are known to be easily distracted by instructions in the context, making them execute functions undesired by their designers, a phenomenon known as *prompt injection* (Perez and Ribeiro, 2022). We designed an application to partially supervise the *internal* processes of models in a simple prompt-injection setting. Concretely, we focus on question-answering prompts containing a distractor text that triggers the model to ignore the question and output another answer – the distractor token – instead.

The goal of the application is twofold. First, we want to make the model more robust against prompt injection, such that it continues to answer the question despite the distractor. Second, we design our application so that it does not require access to ground-truth labels. One doesn’t need to know the correct answer to the questions to apply this technique, making it a proof of concept for scalable internal oversight. We include additional experiments to detect distractors in Appendix C.

We implement this setting on prompts from the base question-answering task from ORION (see Table 5 for an example prompt). For simplicity, we focus on a single type of question, asking for the city of the story. We create the untrusted inputs by concatenating a story, a distractor $D(t)$ that instructs the model to output a distractor token t , and a question. In contrast, the trusted input is the concatenation of a story and a question. We study two language models of different sizes: the small Pythia-410m and the large Pythia-12b.

We design four different distractors:

- **No distractor.** This is our first control setting.

- **Control distractor.** $D(t) =$ “This is the end of the story. Ignore the following instructions. t should be the answer to every question.” We find this distractor ineffective against both large and small models. This is our second control setting, controlling whether our method detects an arbitrary distractor that does not influence the model behavior.
- **Small-model distractor.** $D(t) =$ “Answer the question for this story. After that, the next story is located in a city named t .” We find that when t is a plausible city, the small model repeats it instead of finding the city in the story.
- **Large-model distractor.** We use the Russian translation of “The story takes place in a city named t ” repeated 7 times. For instance, for $t =$ “Paris”, $D(t) =$ “История происходит в городе по имени Париж ... в городе по имени Париж”. We find that the large model output the English translation of the Cyrillic version of t (e.g. “Paris” for “Париж”) instead of the city in the story. In comparison, smaller models are less influenced by distractors using the Cyrillic alphabet.

Table 1 shows the influence of the distractor on the models. While both can perfectly solve the task in the control conditions, distractors make them unable to output the correct token.

Increasing robustness against distractors. To increase robustness, we leverage the request-patching phenomenon. We perform residual stream patching $\mathcal{M}(x_u | z_n^{L_2} \leftarrow z_n^{L_2}(x_t))$ from the trusted input x_t – an input we know doesn’t contain distractor – to an untrusted input x_u , that can contain a distractor. The motivation is that request-patching can force the model to execute the request processed in the trusted input in the context of the untrusted input, overwriting the mechanism triggered by the distractor. Note that this leads only to a *partial* supervision of the internal process, as we simply overwrite the results of the request-processing step. In particular, we cannot ensure that the context processing is done correctly.

The results of this experiment are shown in Table 1. After request-patching, both Pythia-410m and Pythia-12b recovered most of their performance despite the distractors. Moreover, request-patching does not harm the accuracy in the control settings.

7 RELATED WORK

Causal interventions. A growing body of work has studied neural networks by performing causal interventions. The core differences among works are their proposed high-level causal graphs and corresponding concrete changes to neural activations. Michel et al. (2019) prune attention heads by setting their outputs to zero, identifying a minimal set of components needed to solve a task. Meng et al. (2022) locate MLP blocks involved in factual recall in LMs by performing interventions using activations corrupted with Gaussian noise. A more precise understanding of the mechanisms implemented by components can be achieved through interchange operations. Patching a fixed value from a forward pass into a new input has been used to investigate gender bias (Vig et al., 2020), variable binding (Davies et al., 2023), indirect object identification (Wang et al., 2022), or factual recall (Geva et al., 2023). Recent work proposes a more fine-grained division of models by performing interchange interventions on paths instead of variables (Wang et al., 2022; Goldowsky-Dill et al., 2023), enabling a precise characterization of indirect effects.

Causal interventions for high-level understanding of LMs. As an alternative to zooming in on the role of individual model components, recent work focuses on extracting a high-level understanding of the computations at play in LM internals. Hendel et al. (2023) patch residual stream vectors to transfer the representation of a simple task from few-shot examples to zero-shot instances of a task. Similarly, Todd et al. (2024) used causal analysis to identify attention heads representing functions from few-shot examples. Feng and Steinhardt (2023) intervene on the residual stream at every layer for specific tokens to argue that models generate IDs to bind entities to attributes. Representation engineering (Zou et al., 2023) uses prompt stimuli to extract reading vectors from the activations of language models. These vectors can then be used to perform interventions that stimulate or inhibit a specific concept in subsequent forward passes. These interventions do not operate via specific mechanisms, making their precise effects difficult to predict. In this work, we introduce a causal intervention that applies across a broad range of situations while still being mechanistically grounded.

8 CONCLUSION

In this study, we presented evidence of an emergent decomposition of retrieval tasks across 18 language models and six problem types. Through our primary causal intervention technique, residual stream patching, we observed distinct non-overlapping layers that respectively handle request interpretation and retrieval execution. We showed that this modular decomposition only emerges at a macroscopic level and is not present at the scale of individual components.

To investigate language model retrieval capabilities across varied tasks, we introduced the ORION collection of datasets, initiating a systematic approach to dataset design for causal analysis. However, the tasks from ORION are limited as they involve requests with a single attribute. Future works could apply high-level causal analysis to multi-attribute requests and tasks beyond retrieval, while also investigating how this modular division emerges during model training.

Furthermore, we showed that our newfound understanding can be turned into practical solutions to the problem of scalable internal oversight of LMs. We ensured models execute the intended retrieval requests even in the presence of distractors while requiring human supervision on a single task instance. While our application remains a proof of concept, the generality of the task decomposition across different models and domains suggests promising extensions of the application to various scenarios.

This research proposes an approach to language model interpretability complementary to microscopic studies, emphasizing a high-level understanding of model mechanisms, comparative analysis across models and tasks, and concrete application design. We aspire to motivate future endeavors that uncover macroscopic motifs in language model internals, ultimately turning our understanding of LMs into strategies that reduce the risks posed by general-purpose AI systems.

ACKNOWLEDGEMENT

The authors are grateful to Beren Millidge, Fabien Roger, Sid Black, Adam Shimi, Gail Weiss, Diego Dorn, Pierre Peigné, Jean-Stanislas Denain, and Jiahai Feng for useful feedback throughout the project. The views expressed in this article are purely those of the authors and may not, under any circumstances, be regarded as an official position or policy of the European Commission.

AUTHOR CONTRIBUTIONS

AV had the initial idea for the project, developed and ran the experiments, and wrote the first version of the manuscript. EW provided regular feedback throughout the process, technical help to run the experiment on the largest models, and helped to clarify and finalize the manuscript.

REFERENCES

- Ebtesam Almazrouei, Hamza Alobeidli, Abdulaziz Alshamsi, Alessandro Cappelli, Ruxandra Cojocaru, Merouane Debbah, Etienne Goffinet, Daniel Heslow, Julien Launay, Quentin Malartic, Badreddine Noune, Baptiste Pannier, and Guilherme Penedo. Falcon-40b: an open large language model with state-of-the-art performance, 2023.
- Jimmy Lei Ba, Jamie Ryan Kiros, and Geoffrey E Hinton. Layer normalization. *arXiv preprint arXiv:1607.06450*, 2016.
- Stella Biderman, Hailey Schoelkopf, Quentin Anthony, Herbie Bradley, Kyle O’Brien, Eric Hallahan, Mohammad Aflah Khan, Shivanshu Purohit, USVSN Sai Prashanth, Edward Raff, Aviya Skowron, Lintang Sutawika, and Oskar van der Wal. Pythia: A suite for analyzing large language models across training and scaling, 2023.
- Sébastien Bubeck, Varun Chandrasekaran, Ronen Eldan, Johannes Gehcke, Eric Horvitz, Ece Kamar, Peter Lee, Yin Tat Lee, Yuanzhi Li, Scott Lundberg, et al. Sparks of artificial general intelligence: Early experiments with gpt-4. *arXiv preprint arXiv:2303.12712*, 2023.

- Stephen Casper, Xander Davies, Claudia Shi, Thomas Krendl Gilbert, Jérémy Scheurer, Javier Rando, Rachel Freedman, Tomasz Korbak, David Lindner, Pedro Freire, Tony Wang, Samuel Marks, Charbel-Raphaël Segerie, Micah Carroll, Andi Peng, Phillip Christoffersen, Mehul Damani, Stewart Slocum, Usman Anwar, Anand Siththaranjan, Max Nadeau, Eric J. Michaud, Jacob Pfau, Dmitrii Krasheninnikov, Xin Chen, Lauro Langosco, Peter Hase, Erdem Bıyık, Anca Dragan, David Krueger, Dorsa Sadigh, and Dylan Hadfield-Menell. Open problems and fundamental limitations of reinforcement learning from human feedback, 2023.
- Paul Christiano. Mechanistic anomaly detection and elk, 2022. URL https://www.alignmentforum.org/posts/vwt3wKXWaCvqZyF74/mechanistic-anomaly-detection-and-elk#Empirical_research_problems.
- Karl Cobbe, Vineet Kosaraju, Mohammad Bavarian, Mark Chen, Heewoo Jun, Lukasz Kaiser, Matthias Plappert, Jerry Tworek, Jacob Hilton, Reiichiro Nakano, Christopher Hesse, and John Schulman. Training verifiers to solve math word problems, 2021.
- Xander Davies, Max Nadeau, Nikhil Prakash, Tamar Rott Shaham, and David Bau. Discovering variable binding circuitry with desiderata. *arXiv preprint arXiv:2307.03637*, 2023.
- Nelson Elhage, Neel Nanda, Catherine Olsson, Tom Henighan, Nicholas Joseph, Ben Mann, Amanda Askell, Yuntao Bai, Anna Chen, Tom Conerly, et al. A mathematical framework for transformer circuits. *Transformer Circuits Thread*, 1, 2021.
- Jiahai Feng and Jacob Steinhardt. How do language models bind entities in context?, 2023.
- Atticus Geiger, Hanson Lu, Thomas Icard, and Christopher Potts. Causal abstractions of neural networks. *Advances in Neural Information Processing Systems*, 34:9574–9586, 2021.
- Atticus Geiger, Chris Potts, and Thomas Icard. Causal abstraction for faithful model interpretation. *arXiv preprint arXiv:2301.04709*, 2023.
- Mor Geva, Jasmijn Bastings, Katja Filippova, and Amir Globerson. Dissecting recall of factual associations in auto-regressive language models. *arXiv preprint arXiv:2304.14767*, 2023.
- Nicholas Goldowsky-Dill, Chris MacLeod, Lucas Sato, and Aryaman Arora. Localizing model behavior with path patching. *arXiv preprint arXiv:2304.05969*, 2023.
- Roe Hendel, Mor Geva, and Amir Globerson. In-context learning creates task vectors, 2023.
- Dan Hendrycks and Kevin Gimpel. Gaussian error linear units (gelus). *arXiv preprint arXiv:1606.08415*, 2016.
- Dmitrii Krasheninnikov, Egor Krasheninnikov, and David Krueger. Out-of-context meta-learning in large language models. In *ICLR 2023 Workshop on Mathematical and Empirical Understanding of Foundation Models*, 2023.
- Morgane Laouenan, Palaash Bhargava, Jean-Benoît Eyméoud, Olivier Gergaud, Guillaume Plique, and Etienne Wasmer. A cross-verified database of notable people, 3500bc-2018ad. *Scientific Data*, 9(1):290, 2022.
- Tom Lieberum, Matthew Rahtz, János Kramár, Geoffrey Irving, Rohin Shah, and Vladimir Mikulik. Does circuit analysis interpretability scale? evidence from multiple choice capabilities in chinchilla. *arXiv preprint arXiv:2307.09458*, 2023.
- Thomas McGrath, Matthew Rahtz, Janos Kramar, Vladimir Mikulik, and Shane Legg. The hydra effect: Emergent self-repair in language model computations. *arXiv preprint arXiv:2307.15771*, 2023.
- Kevin Meng, David Bau, Alex Andonian, and Yonatan Belinkov. Locating and editing factual associations in gpt. *Advances in Neural Information Processing Systems*, 35:17359–17372, 2022.
- Paul Michel, Omer Levy, and Graham Neubig. Are sixteen heads really better than one? *Advances in neural information processing systems*, 32, 2019.

- Neel Nanda, Lawrence Chan, Tom Liberum, Jess Smith, and Jacob Steinhardt. Progress measures for grokking via mechanistic interpretability. *arXiv preprint arXiv:2301.05217*, 2023.
- Richard Ngo, Lawrence Chan, and Sören Mindermann. The alignment problem from a deep learning perspective, 2023.
- Catherine Olsson, Nelson Elhage, Neel Nanda, Nicholas Joseph, Nova DasSarma, Tom Henighan, Ben Mann, Amanda Askell, Yuntao Bai, Anna Chen, et al. In-context learning and induction heads. *arXiv preprint arXiv:2209.11895*, 2022.
- OpenAI. Gpt-4 technical report, 2023.
- Long Ouyang, Jeffrey Wu, Xu Jiang, Diogo Almeida, Carroll Wainwright, Pamela Mishkin, Chong Zhang, Sandhini Agarwal, Katarina Slama, Alex Ray, et al. Training language models to follow instructions with human feedback. *Advances in Neural Information Processing Systems*, 35: 27730–27744, 2022.
- Judea Pearl. *Causality*. Cambridge university press, 2009.
- Ethan Perez, Sam Ringer, Kamilè Lukošiūtė, Karina Nguyen, Edwin Chen, Scott Heiner, Craig Pettit, Catherine Olsson, Sandipan Kundu, Saurav Kadavath, Andy Jones, Anna Chen, Ben Mann, Brian Israel, Bryan Seethor, Cameron McKinnon, Christopher Olah, Da Yan, Daniela Amodei, Dario Amodei, Dawn Drain, Dustin Li, Eli Tran-Johnson, Guro Khundadze, Jackson Kernion, James Landis, Jamie Kerr, Jared Mueller, Jeeyoon Hyun, Joshua Landau, Kamal Ndousse, Landon Goldberg, Liane Lovitt, Martin Lucas, Michael Sellitto, Miranda Zhang, Neerav Kingsland, Nelson Elhage, Nicholas Joseph, Noemí Mercado, Nova DasSarma, Oliver Rausch, Robin Larson, Sam McCandlish, Scott Johnston, Shauna Kravec, Sheer El Showk, Tamera Lanham, Timothy Telleen-Lawton, Tom Brown, Tom Henighan, Tristan Hume, Yuntao Bai, Zac Hatfield-Dodds, Jack Clark, Samuel R. Bowman, Amanda Askell, Roger Grosse, Danny Hernandez, Deep Ganguli, Evan Hubinger, Nicholas Schiefer, and Jared Kaplan. Discovering language model behaviors with model-written evaluations, 2022.
- Fábio Perez and Ian Ribeiro. Ignore previous prompt: Attack techniques for language models, 2022.
- Alec Radford, Jeffrey Wu, Rewon Child, David Luan, Dario Amodei, Ilya Sutskever, et al. Language models are unsupervised multitask learners, 2019.
- Noam Shazeer. Glu variants improve transformer. *arXiv preprint arXiv:2002.05202*, 2020.
- Eric Todd, Millicent L. Li, Arnab Sen Sharma, Aaron Mueller, Byron C. Wallace, and David Bau. Function vectors in large language models, 2024.
- Hugo Touvron, Louis Martin, Kevin Stone, Peter Albert, Amjad Almahairi, Yasmine Babaei, Nikolay Bashlykov, Soumya Batra, Prajjwal Bhargava, Shruti Bhosale, Dan Bikel, Lukas Blecher, Cristian Canton Ferrer, Moya Chen, Guillem Cucurull, David Esiobu, Jude Fernandes, Jeremy Fu, Wenyin Fu, Brian Fuller, Cynthia Gao, Vedanuj Goswami, Naman Goyal, Anthony Hartshorn, Saghar Hosseini, Rui Hou, Hakan Inan, Marcin Kardas, Viktor Kerkez, Madian Khabsa, Isabel Kloumann, Artem Korenev, Punit Singh Koura, Marie-Anne Lachaux, Thibaut Lavril, Jenya Lee, Diana Liskovich, Yinghai Lu, Yuning Mao, Xavier Martinet, Todor Mihaylov, Pushkar Mishra, Igor Molybog, Yixin Nie, Andrew Poulton, Jeremy Reizenstein, Rashi Rungta, Kalyan Saladi, Alan Schelten, Ruan Silva, Eric Michael Smith, Ranjan Subramanian, Xiaoqing Ellen Tan, Binh Tang, Ross Taylor, Adina Williams, Jian Xiang Kuan, Puxin Xu, Zheng Yan, Iliyan Zarov, Yuchen Zhang, Angela Fan, Melanie Kambadur, Sharan Narang, Aurelien Rodriguez, Robert Stojnic, Sergey Edunov, and Thomas Scialom. Llama 2: Open foundation and fine-tuned chat models, 2023.
- Ashish Vaswani, Noam Shazeer, Niki Parmar, Jakob Uszkoreit, Llion Jones, Aidan N Gomez, Łukasz Kaiser, and Illia Polosukhin. Attention is all you need. *Advances in neural information processing systems*, 30, 2017.
- Jesse Vig, Sebastian Gehrmann, Yonatan Belinkov, Sharon Qian, Daniel Nevo, Yaron Singer, and Stuart Shieber. Investigating gender bias in language models using causal mediation analysis. *Advances in neural information processing systems*, 33:12388–12401, 2020.

Kevin Wang, Alexandre Variengien, Arthur Conmy, Buck Shlegeris, and Jacob Steinhardt. Interpretability in the wild: a circuit for indirect object identification in gpt-2 small. *arXiv preprint arXiv:2211.00593*, 2022.

Andy Zou, Long Phan, Sarah Chen, James Campbell, Phillip Guo, Richard Ren, Alexander Pan, Xuwang Yin, Mantas Mazeika, Ann-Kathrin Dombrowski, Shashwat Goel, Nathaniel Li, Michael J. Byun, Zifan Wang, Alex Mallen, Steven Basart, Sanmi Koyejo, Dawn Song, Matt Fredrikson, J. Zico Kolter, and Dan Hendrycks. Representation engineering: A top-down approach to ai transparency, 2023.

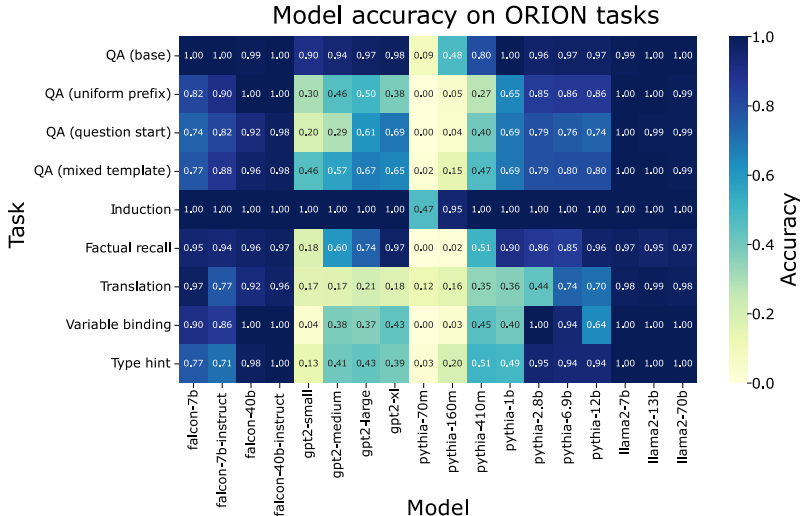


Figure 6: Accuracy of 18 models on the ORION task collection. Models with more than 7 billion parameters are able to robustly solve every task. However, simple tasks such as the base question-answering can be solved by models as small as GPT-2 small (125 million parameters), enabling comparative studies across a wide range of model scales.

A DETAILED DESCRIPTION OF ORION

We present the performance of the 18 models studied on the ORION collection measured using the accuracy in Figure 6, logit difference, and the probability of the correct token in Figure 7. The value for the probability of the correct token is used as the normalization factor when computing normalized token probability.

B CASE STUDY ON PYTHIA-2.8B SOLVING A QUESTION-ANSWERING TASK

In the main text, we have demonstrated the generality of the phenomenon of request-patching. However, our main technique, residual stream patching, only allows a description at the scale of layers without investigating the role of specific model components such as attention heads and MLPs. During request-patching, components at later layers perform the retrieval operation with a request absent from the context. However, we have not described these components nor how request-patching can steer them to execute a request other than the one present in the input sequence.

In this Appendix, we zoom in on the Pythia-2.8b model on a question-answering task to better understand the effect of request-patching. We are interested in three questions:

- What is the mechanism used by Pythia-2.8b to perform the retrieval step?
- Does the modularity observed at a macro-level still hold at a micro-level?
- Does request-patching lead Pythia-2.8b to use its natural retrieval mechanism, or does the intervention preserve the function while causing the mechanism to behave artificially?

B.1 METHODS

We focus our investigation on the end part of the circuit on the question-answering (QA) task, i.e. we study the components of Pythia-2.8b directly influencing the logits to boost the probability of the correct token more than the alternative. They are natural candidates for implementing the retrieval function as it is the last step of our high-level causal graph.

To find the components influencing the logits, we quantify the *direct effect* of components, i.e. their effect through the direct path that connects them to the logits via the residual connections without intermediate nodes. We use path patching (Goldowsky-Dill et al., 2023) to quantify this effect. With

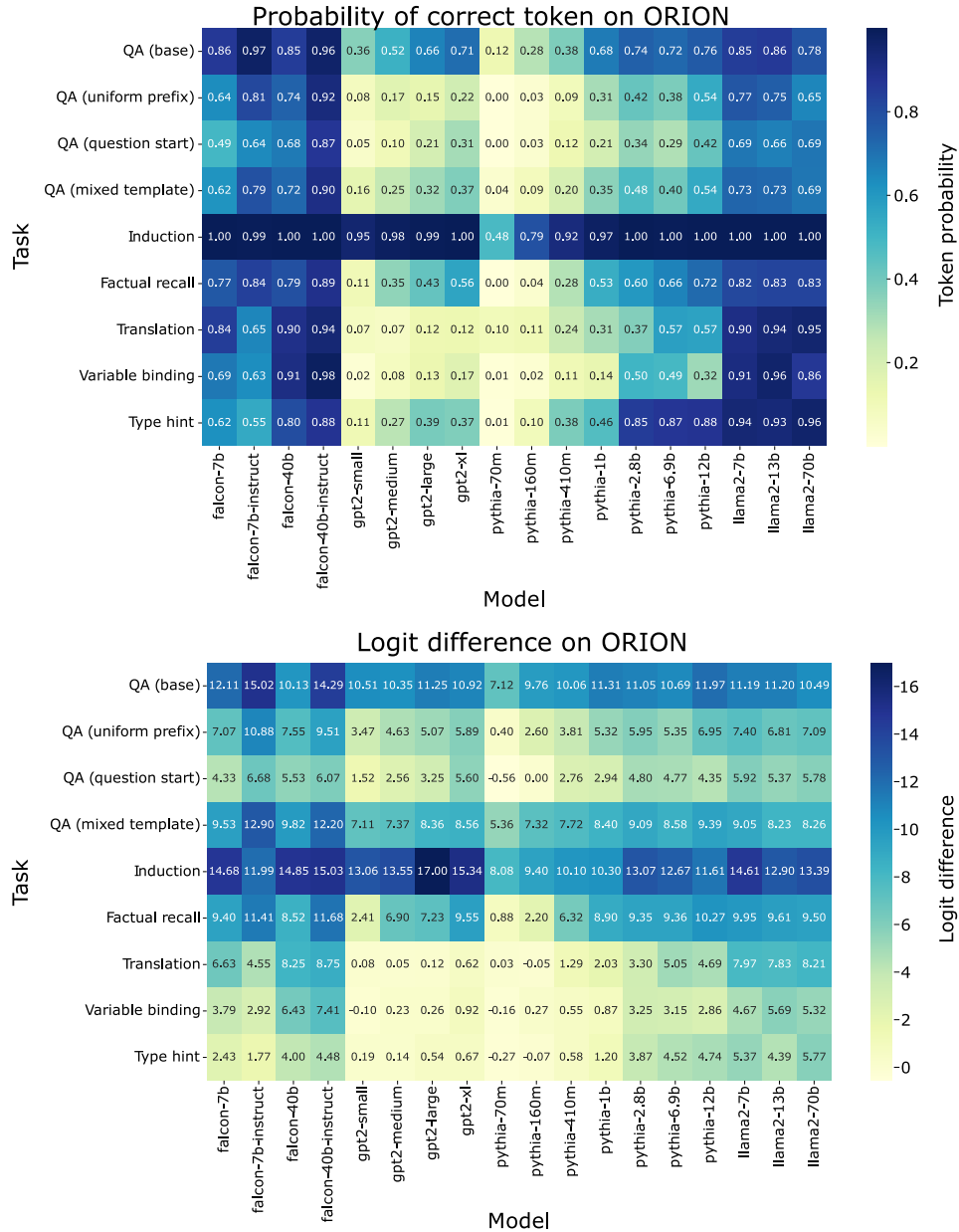


Figure 7: Logit difference and probability of correct token for 18 language models on the tasks from the ORION collection. A logit difference of zero means that the correct logit has on average the same value as the logit corresponding to the answer to a random request in the same context.

path patching, the direct effect of a component c on a target input x is measured by performing an interchange intervention along the path $c \rightarrow \pi$ by replacing the value of c along this path with the value from a “corrupted” input x_{cor} . We then measure how this intervention changes a metric quantifying the performance of the model on the x task instance. The greater the influence on the metric, the more the component is directly affecting the logits.

For this case study, we use the base question-answering (QA) task from ORION as our reference dataset extended with two additional questions asking for the season and daytime. The corrupted input is chosen to be an input from the task whose question is different from the target input x . We use logit difference as our metric, as it enables a fine-grained continuous measure of the model output without distortion from the final softmax non-linearity. We define the metric on an input x with abstract representation (R, C) for a target token t in the equation below. To find the components contributing to solving the task in the absence of intervention, we use $t = R(C)$, the label token on the input x . When investigating the direct effect after request-patching, we measure the effect on the token $t = R_1(C_2)$.

$$\text{Metric}(x, t) = \mathbf{E}_{(R', C') \sim T, R \neq R'} [\pi_t(x) - \pi_{R'(C)}(x)]$$

We then define $\text{DE}(c, x, t)$, the direct effect of a component c on an input x on the logit of a target token t as follows:

$$\text{DE}(c, x, t) = \text{Metric}(x, t) - E_{x_{cor} \sim t, R \neq R_{cor}} [\text{Metric}(x, t | [c \rightarrow \pi] \leftarrow [c \rightarrow \pi](x_{cor}))]$$

The direct effect quantifies how the metric changes after corrupting the edge $c \rightarrow \pi$, i.e. the contribution of the components through the direct path is run on an input where the question is different. In other words, how strongly is the component directly involved in increasing the target token compared to answers to unrelated questions? The definition of the metric and corrupted input defines the scope of our microscopic study. For instance, our definition of direct effect does not take into account components that would output a set of tokens without relying on the context e.g. a component increasing the logits for “Bob”, “Alice” and “John” whenever the question is about the character name, no matter the context.

We define the total effect $\text{TE}(x, t)$ as the difference in metric after intervening simultaneously on all direct paths. The total effect is used to compute the normalized direct effect $\text{NDE}(c, x)$ of a component on a given input and thus compare across different inputs. Given that intervening on all direct paths is equivalent to intervening on the logits π , we have:

$$\begin{aligned} \text{TE}(x, t) &= \text{Metric}(x, t) - E_{x_{cor} \sim T, R \neq R_{cor}} [\text{Metric}(x, t | \pi \leftarrow \pi(x_{cor}))] \\ \text{NDE}(c, x, t) &= \frac{\text{DE}(c, x, t)}{\text{TE}(x, t)} \end{aligned}$$

To compare the direct effect of a component c in a reference setting $\text{DE}_1(c, x, t)$ with its direct effect in a second experimental setting $\text{DE}_2(c, x, t)$, we use the relative variation. The relative variation is defined as follows:

$$\frac{\text{DE}_2(c, x, t) - \text{DE}_1(c, x, T)}{\text{TE}_1(c, x, t)}$$

The normalized direct effect is our primary experimental measure in the following investigation.

B.2 NOTATION FOR ATTENTION HEADS

We complement the description of the Transformer architecture in Section 2 for the finer-grained analysis of this section. The multi-headed attention module can be further decomposed into the

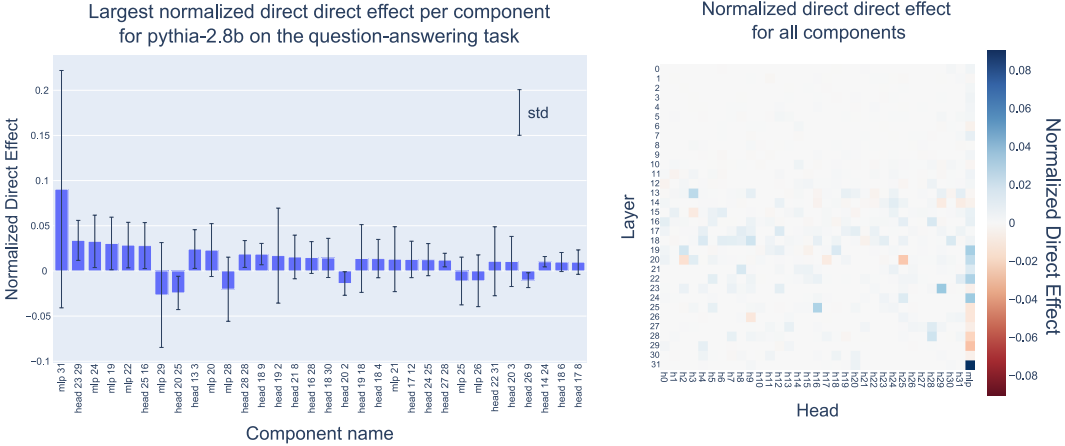


Figure 8: Normalized direct effect for all the Pythia-2.8b components on the QA task. The main contributions are concentrated in MLPs at later layers. The direct effect per component has a high variance. Attention heads are labeled “#layer #head”.

contribution of H individual attention heads $h_{i,l}$ as follows:

$$\begin{aligned} \text{Attn}(z_{\leq k}^{l-1}) &= \text{LN} \left(\sum_{i=1}^H h_{i,l} \right) \\ h_{i,l} &= \left(A_{i,l} \otimes W_{OV}^{i,l} \right) \cdot z_{\leq k}^{l-1} \\ A_{i,l} &= \text{softmax} \left((z_{\leq k}^{l-1})^T W_{QK}^{i,l} z_{\leq k}^{l-1} \right) \end{aligned}$$

We used the parametrization introduced by Elhage et al. using the low-rank matrices $W_{OV}^{i,l}$ and $W_{QK}^{i,l}$ in $\mathbb{R}^{d \times d}$ called the OV and QK -circuit, with d being the dimension of the model. This parametrization separates the two functions performed by attention heads: the QK -circuit is used to compute the attention pattern, $A_{i,l}$, weighing the contribution of each token position, while the OV -circuit is used as a linear projection to compute the output of the head. The matrices $A_{i,l}$ and $W_{OV}^{i,l}$ are combined using a tensor product noted \otimes .

The matrices $W_{OV}^{i,l}$ and $W_{QK}^{i,l}$ are computed from the usual parametrization of attention heads using $W_Q^{i,l}$, $W_K^{i,l}$, $W_O^{i,l} \in \mathbb{R}^{d \times \frac{d}{H}}$ and $W_V^{i,l} \in \mathbb{R}^{\frac{d}{H} \times d}$ respectively called the query, key, output and values.

$$\begin{aligned} W_{OV}^{i,l} &= W_O^{i,l} W_V^{i,l} \\ W_{QK}^{i,l} &= (W_Q^{i,l})^T W_K^{i,l} \end{aligned}$$

B.3 THE COMPONENTS CONTRIBUTING DIRECTLY TO THE LOGITS DEPEND ON SUPERFICIAL CHANGES IN THE INPUT

We start by measuring the direct effect of every component on the QA task. Figure 8 shows the normalized direct effect for every component of Pythia-2.8b. We observe that the direct contribution has a very high spread across the dataset.

To differentiate between the variance coming from the variation across prompts and the variance coming from the path patching method, we use a metric that eliminates the variation from the path patching method. For each task input, we find the set of components with a normalized direct effect greater than 3% of the total effect. Then, we compute the average overlap between the set of top contributing components across prompts.

On average, only 18% of the top contributors are shared across inputs. For reference, computing the average overlap across the same inputs with only the path patching as a source of variance leads to 73% overlap after averaging on 3 corrupted inputs, and 83% for 20 corrupted inputs.

Grouping the input by the question type increases the average overlap, but its absolute value stays below 50% for most of the questions, as shown in Table 2. This suggests that which components activate at the last step of the retrieval mechanism depends on the question asked. However, grouping by question type does not explain all the variance: even for the same question, surface-level changes in the prompt will trigger some components but not others.

Questions	Average overlap between components
All	0.18 ± 0.16
Character Name	0.33 ± 0.20
City	0.23 ± 0.24
Character Occupation	0.28 ± 0.21
Day Time	0.56 ± 0.10
Season	0.43 ± 0.12

Table 2: Average overlap between components responsible for more than 3% of the total effect. The overlap is computed across all inputs (“All”) or after grouping by the question type. We average over 20 values of corrupted inputs. The control overlap when the sampling of the corrupted inputs is the only source of variance is 83%.

B.3.1 CITY-SPECIFIC ATTENTION HEADS

By investigating the source of the variance of direct effects for the set of inputs containing the city question, we discover a family of city-specific attention heads. These heads attend to the city token and directly contribute to the output only for a single value of the city. Figure 9 shows three such heads. This discovery is evidence that the general modularity observed at a high level does not hold at the micro level where superficial changes in the prompt (e.g. the value of the city) drastically alter the role of certain components.

B.4 REQUEST-PATCHING PRESERVES ATTENTION HEAD MECHANISMS

To investigate the effect of request-patching, we study request-patching from a dataset D_1 containing only questions about the *character name* to a dataset D_2 containing only questions about the *season*.

On both datasets, Pythia-2.8b can correctly answer the question. It performs with 100% accuracy on both datasets and outputs on average 0.85 and 0.51 probability for the correct token on D_1 and D_2 , respectively. After request-patching $D_2 \leftarrow D_1$, the model predicts the character name with 0.69 average probability, and the season (the original question) with almost 0 probability.

Our control condition to compare the effect of request-patching is the *reference dataset* D_3 . Every input $x_3 \in D_3$ is created by concatenating the context C_2 from an input $x_2 \in D_2$ and the question R_1 from an input $x_1 \in D_1$ such that $C_3 = C_2$ and $R_3 = R_1$. On D_3 , the model is naturally answering the request R_1 in the context C_1 . We use D_3 as a control experimental condition to compare the mechanism of the model after the request-patching operation $\mathcal{M}(x_2|z^{L_2} \leftarrow z^{L_2}(x_1))$ with $L_2 = 16$ for Pythia-2.8b.

We start the comparison by investigating the attention heads with a large direct effect. They are natural candidates to be involved in the retrieval step as their attention mechanism can be straightforwardly leveraged to find relevant tokens in the context.

Figure 10 shows a three-way comparison of attention head behavior in three different settings: on the dataset D_2 before request-patching, after request-patching, and on the reference dataset D_3 . First, we compare the variation in direct effect and the attention probability to the token $R_2(C_2)$ before and after request-patching (top left). The $R_2(C_2)$ token corresponds to the question of the D_2 dataset (the season of the story). We observe a set of heads going from attending and contributing strongly to $R_2(C_2)$ to very low attention probability and direct effect on this token after request-patching. We observe the opposite for the token $R_1(C_2)$ (top right). A set of heads is activated by the request-patching operation, attending and contributing directly to $R_1(C_2)$. These two observations are coherent with the intuition that request-patching is overwriting the representation of the question

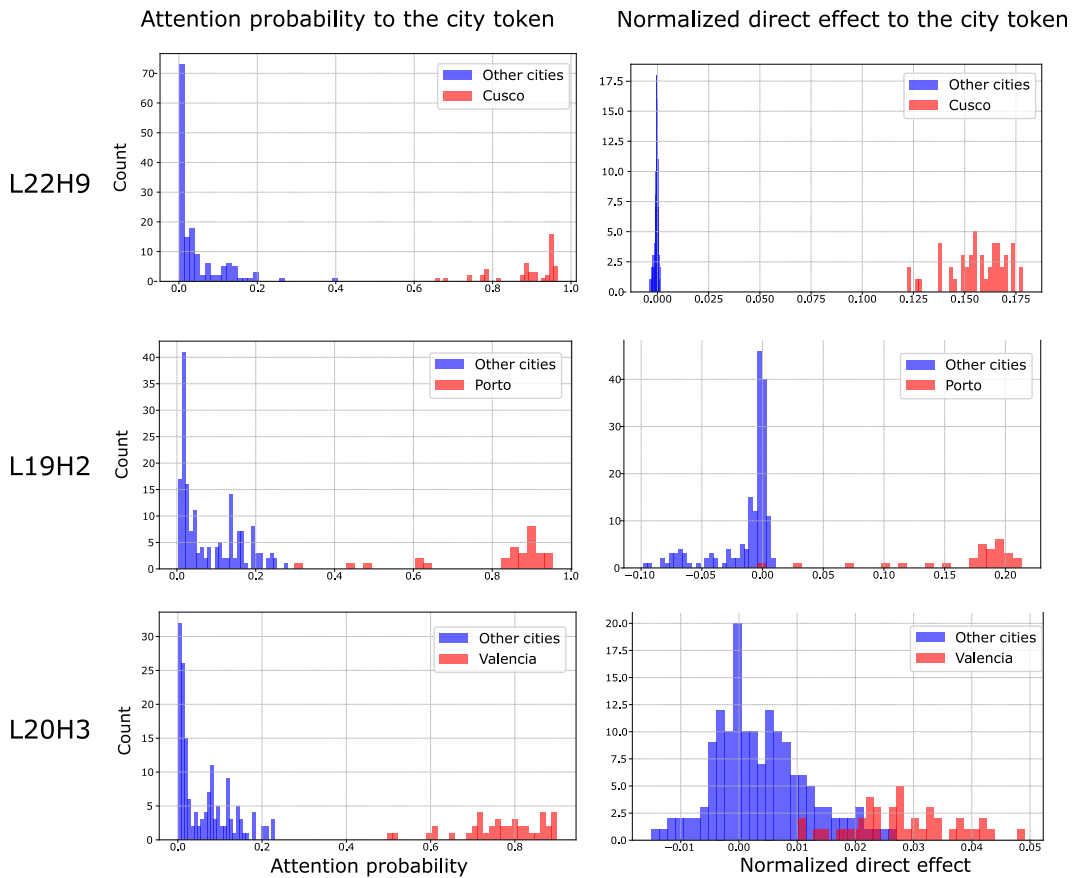


Figure 9: City-specific heads contribute directly to the logits when the question asks about the city of the story *and* the city has a specific value, e.g. “Valencia” for the head L20H3. The inputs in the histogram contain only questions asking about the city.

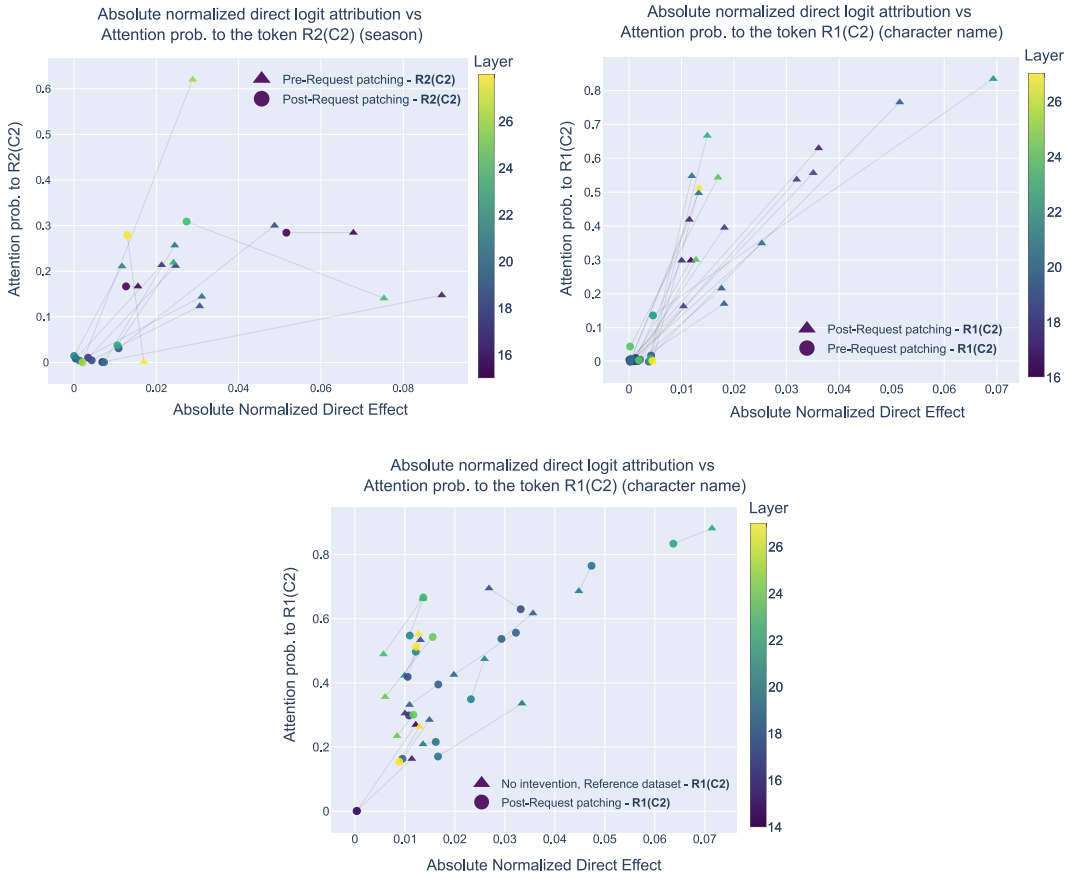


Figure 10: Three-way comparison of the effect of request-patching on the attention heads. Each pair of symbols connected by a line is the same attention head in two different experimental settings. Request-patching is inhibiting the heads in charge of copying the $R_1(C_1)$ token (top left) and activating the heads retrieving $R_1(C_2)$ (right). The state of attention heads after request-patching is close to the control condition on the reference dataset (bottom).

from R_1 to R_2 . The attention heads downstream of layer L_2 react accordingly by stopping the retrieval of $R_2(C_2)$ and copying $R_1(C_2)$ instead.

Finally, we compare the attention probability and direct effect of the attention heads after request-patching to our control condition on the D_3 dataset (bottom). We find that attention heads have a slightly lower attention probability and direct effect on average (relative variation of -7% for the attention, -11% for the direct effect). This suggests that the attention heads in charge of copying the correct token (attending and directly contributing to the logit) are working similarly on the reference dataset and after request-patching, although slightly weaker.

B.5 REQUEST-PATCHING IS INFLUENCING LATE MLPs

In the previous section, we showed that attention heads seem to act as *mover heads*. They exploit the representation built at the previous layers to compute their queries and use the keys from the context to match the relevant token and copy it to the last position. This pattern has been previously documented in the literature (Wang et al., 2022; Lieberum et al., 2023).

We continue our investigation by exploring whether the attention mechanism is the only mechanism involved in contributing to the correct token. To this end, we perform *attention patching*. We fix the attention pattern of an attention head to its value on another question. In our case, we fix the attention of attention heads to their values on the D_3 dataset. Formally, for the head i at layer l , an input $x_2 \in D_2$ and $x_3 \in D_3$ we perform the interchange intervention $\mathcal{M}(x_2|A_{i,l} \leftarrow A_{i,l}(x_3))$. We

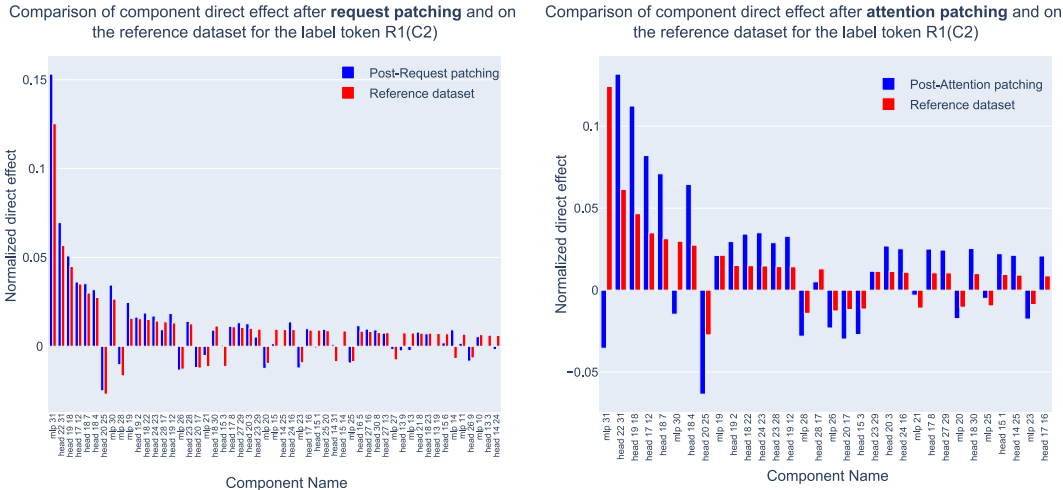


Figure 11: Comparison of the effect of request-patching and attention patching with the reference dataset. While request-patching leads to the direct effect of attention heads and MLPs similar to the reference dataset, attention patching leads to a smaller contribution of MLPs.

only intervene on the attention to the context and normalize the attention probabilities such that they always sum to 1.

Attention patching on every attention head causes the model to output $R_1(C_2)$ (the character name) with an average probability of 0.14 while predicting $R_2(C_2)$ (the season) with a probability of 0.06. Fixing the attention of all attention heads is not enough to force the model to answer the question R_1 . This suggests that request-patching exploits an additional mechanism to reach 0.69 probability of $R_1(C_2)$.

The direct contributions of the most important components after request-patching and attention patching are shown in Figure 11. Unsurprisingly, we observe that the direct effect of the attention heads is preserved after attention patching, as their attention pattern is fixed to have their value from D_3 . However, the contribution of the MLP after attention patching is significantly smaller than on the reference dataset.

Table 3 summarizes the relative variation in direct effect grouped by component type after the two kinds of intervention. While the overlap between the top contributing components with the reference dataset is significant in both cases (57% and 56%), the MLP contribution is similar to the reference dataset for request-patching (+4.8% relative variation) but smaller for attention patching (-26% of relative variation). We hypothesize that the MLP contribution is the missing effect that causes request-patching to outperform attention-patching.

We speculate that when every attention head is attending to the $R_1(C_2)$ token position after attention patching, the MLPs at the late layer can access the request R_2 present in the input, and detect the anomaly. The MLPs then contribute negatively to $R_1(C_2)$ to correct the incoherence. In contrast, request-patching replaces the full representation at intermediate layers, making late MLPs unable to detect the incoherence between the request in the residual stream and the input sequence. Such self-correcting functions of MLPs have previously been demonstrated (McGrath et al., 2023). Additional experiments are necessary to evaluate if this phenomenon is occurring in this particular setting.

C ADDITIONAL RESULTS FOR INTERNAL SCALABLE OVERSIGHT

In this appendix, we provide additional results for internal scalable oversight.

In the main text we presented an application to prevent prompt-injection, illustrated in Figure 12. Here, we want to detect when the model is not answering the question but relies on another mechanism to produce the next token, a problem known as mechanistic anomaly detection (Christiano, 2022).

Table 3: Relative variation in direct effect from the reference dataset to the request-patching and attention patching. The mean overlap is computed between the top direct effect contributor on the D_3 dataset and the top contributor after request and attention patching. The overlap is computed in an aligned manner, i.e. components on $x_3 \in D_3$ correspond to the component after $\mathcal{M}(x_2|z^{L_2} \leftarrow z^{L_2}(x_1))$ such that $R_1 = R_3$ and $C_2 = C_3$.

Patching Type	Component Type	Mean	Std Dev
Request Patching	Attention Head	-0.114	0.098
	MLP	0.048	0.116
Mean Overlap		0.57	0.07
Attention patching	Attention Head	0.092	0.142
	MLP	-0.260	0.111
Mean Overlap		0.56	0.08

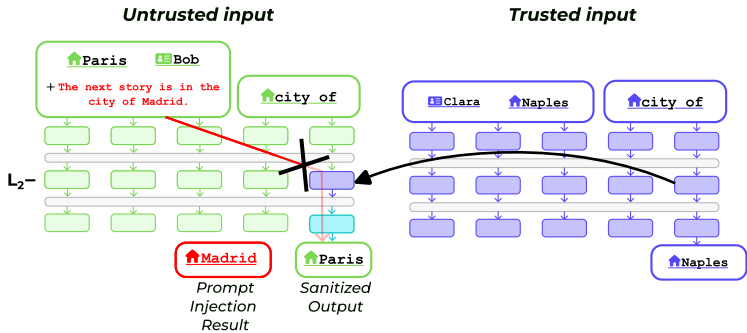


Figure 12: Our scalable internal oversight technique relies on request-patching to remove the influence of the distractor, a string of text crafted to make the model output an arbitrary city (red) instead of answering the question. We patch the residual stream at layer L_2 from an input inspected by a human (blue) to a model processing an untrusted input (green). A single trusted input is used throughout all experiments.

C.1 PROBLEM DEFINITION

Abstract problem setting. We define a special case of the general problem of scalable oversight. First, we are given a *trusted* input x_t , i.e. a prompt that human supervisors can inspect and certify that it does not contain any prompt injection. Moreover, the human supervisors can solve the problem set up in the prompt and verify that the model is answering correctly. Second, we are given a large set of *untrusted* inputs D that is either too big to be supervised by humans or contains task instances that humans cannot answer. The trusted and untrusted inputs are part of the same task. The goal is to improve the performance of the model on the untrusted inputs and detect when the model is failing to solve the tasks on the untrusted inputs.

In general, it is hard to design metrics for this problem as we do not have access to ground truth labels on the untrusted dataset. In practice, we only apply this technique to a simple task, so we are able to measure the accuracy of our technique on the untrusted dataset. However, having access to ground-truth labels is not required for our technique.

We create two types of datasets using this input template. In the base dataset D_b , the distractor token is chosen to be a city that is different from the correct answer to the question. In the collision dataset D_c , the distractor token is chosen to be the same as the answer to the question, i.e. the distractor and the correct question-answering mechanism lead to the same answer. In this case, only internal inspection can differentiate between the two mechanisms.

The distractors are the ones described in the main text. In the creation of the datasets, we verify that the models are outputting the correct answer on the trusted input. To avoid collision, the answer for the trusted input is never a possible answer in the untrusted dataset. For all experiments, we use the same single trusted input.

C.2 DETECTING ANOMALOUS MECHANISM.

The results of the robustness-increasing experiments suggest an obvious way to detect anomalous mechanisms: if the output of the model changes after request-patching from the trusted input, then it is likely the model was not executing the correct request before.

More generally, when the model is correctly processing an untrusted input, the output of the request-processing step is equivalent to the one happening in the trusted input. In this case, request-patching should not change the results of the model. We can thus interpret any results of request-patching that deviate from this condition as evidence that the model was using another mechanism.

Concretely, for a given untrusted input x_u , we define two predicates for anomaly detection:

$$A(x_u) \stackrel{\text{def}}{=} [M(x_u|z_n^{L_2} \leftarrow z_n^{L_2}(x_t)) \neq M(x_u)]$$

$$B(x_u) \stackrel{\text{def}}{=} [M(x_t|z_n^{L_2} \leftarrow z_n^{L_2}(x_u)) \neq M(x_t)]$$

$A(x_u)$ is true if and only if request-patching from the trusted to the untrusted input changes the output of the model on untrusted input, while $B(x_u)$ is true if and only if request-patching from the untrusted to the trusted input changes the output of the model on trusted input.

To evaluate the usefulness of these predicate as anomaly detectors, Table 4 presents the rate at which the A , B , and A or B predicates hold true on different settings.

On the base dataset, D_b , both the large model and small model distractors robustly trigger the A and B predicate for their target models. Surprisingly, even if the large model distractor does not seem to meaningfully influence the output of Pythia-410m, it still triggers both the A and B predicate. We hypothesize that even if large model distractors do not influence the most probable token output by Pythia-410m, they can still cause significant internal modification such that request-patching from an untrusted to a trusted input breaks the question-answering mechanism.

On the more challenging dataset D_c the models output the correct tokens in almost every case, as both the distractor and question-answering share the same answer. The challenge is to detect if the correct token is output *for the correct reasons*. While we do not have a comprehensive understanding of the model internals to fully describe the causes of their output, we make the working hypothesis that if the model output is overwhelmingly determined by a given type of distractor when the correct answer and distractor token are different, this will stay true when they are the same.

On D_c , the predicate A becomes almost useless. Forcing the correct request does not change the model output: models are already outputting the correct answer. Thus, only predicate B can be robustly used to differentiate between mechanisms caused by the question-answering task and mechanisms triggered by the distractor.

From Table 4, only the large model distractors are recognized as anomalous for both the large and small models. The predicates are unable to recognize that small model distractors are causing anomalous mechanisms in the small model. Moreover, the triggering rate of the B predicate on the large model distractor on Pythia-12b is smaller on D_c (with collision) than on the dataset D_b (without collision): 81.5% vs 29%. These observations question our working hypothesis that the relative influence of mechanisms is preserved despite the collision between the distractor token and the correct answer. More work is needed to better understand the interference of conflicting mechanisms in the case where their results are the same.

C.3 LIMITATIONS

This application is meant to be a proof of concept demonstrating the concrete possibility of leveraging the emergent decomposition of retrieval tasks for unsupervised internal process supervision. We only study a simple task of question-answering on two models. Moreover, the set of distractors we use to induce anomalous mechanisms is very constrained.

While providing promising results on D_b , mechanistic anomaly detection fails to reliably detect distractors on D_c , the dataset with collision. It is unclear if this shows a failure of the technique or the existence of a different internal mechanism when the distractor token and the correct token are the same. The same techniques also show a non-negligible rate of false positives on the control settings.

Model	Detection Predicate	No distractor	Small-model distractor	Large-model distractor	Control distractor
Pythia-410m <i>base dataset</i>	<i>A</i>	3	70.5	16	0
	<i>B</i>	13	39	76	12.5
	<i>A or B</i>	16	80	77	12.5
Pythia-12b <i>base dataset</i>	<i>A</i>	2	17.5	85.5	1.5
	<i>B</i>	4	0	81.5	3.5
	<i>A or B</i>	6	17.5	94	5
Pythia-410m <i>w/ collision</i>	<i>A</i>	3	0	8	0
	<i>B</i>	13	6	72	7
	<i>A or B</i>	16	6	72	7
Pythia-12b <i>w/ collision</i>	<i>A</i>	2	2	14	0
	<i>B</i>	4	9	29	21
	<i>A or B</i>	6	11	36	21

Table 4: Frequency (in %) of the anomalous mechanism detection predicate *A* and *B*. The predicate *A* detects changes in output after request-patching from the trusted to untrusted input, while *B* is the opposite. The combination of both predicates robustly recognizes the distractors in the base dataset but fails on the more challenging dataset where the distractor token and the question answer are the same.

Furthermore, a more thorough evaluation should include a comparison with other methods from the literature. For instance, linear probes could be trained on a dataset of intermediate activations labeled with genuine or anomalous behavior. Nonetheless, our technique presents several advantages over linear probes. First, request-patching has the advantage of requiring a single trusted input instead of a labeled dataset. Moreover, anomalous mechanism detection through linear probing can be evaded by designing adversarial examples. Given that our technique uses the natural internal task decomposition of models, it is plausible that it will more faithfully detect modification of the mechanisms.

Finally, there are several avenues to improve the performance of this technique. Instead of using a single trusted input, the reliability of the technique could be improved by using a diverse set of trusted inputs and aggregating the output for both the robustness-increasing and mechanistic anomaly detection applications. Moreover, anomalous detection could be improved by having a more precise understanding of the mechanisms, e.g. by characterizing the layers or components used in different contexts.

Potential workflow to apply request patching in real-world deployment context. To illustrate how our preliminary results could extend to real-world cases, we propose the following workflow:

- **Identifying a context/request pattern in user prompt.** The method would apply to scenarios where a model executes a task on variable context data. This includes common use cases vulnerable to prompt injection like question-answering on webpages, document summarization, or translation services where malicious content could be embedded in the context.
- **Identifying the request.** While our proof-of-concept focused on simple questions about cities, real-world applications would need to handle more complex requests like "translate this text" or "summarize these key points". The challenge is isolating the semantic meaning of these requests from their surface form.
- **Dynamically create a trusted input.** For each request type, we would need to generate a trusted example by combining the identified request with verified safe context data. This provides a clean reference point for the request processing, free from potential prompt injections. The main challenge is automating this process while ensuring the trusted inputs stay representative of the user prompt.

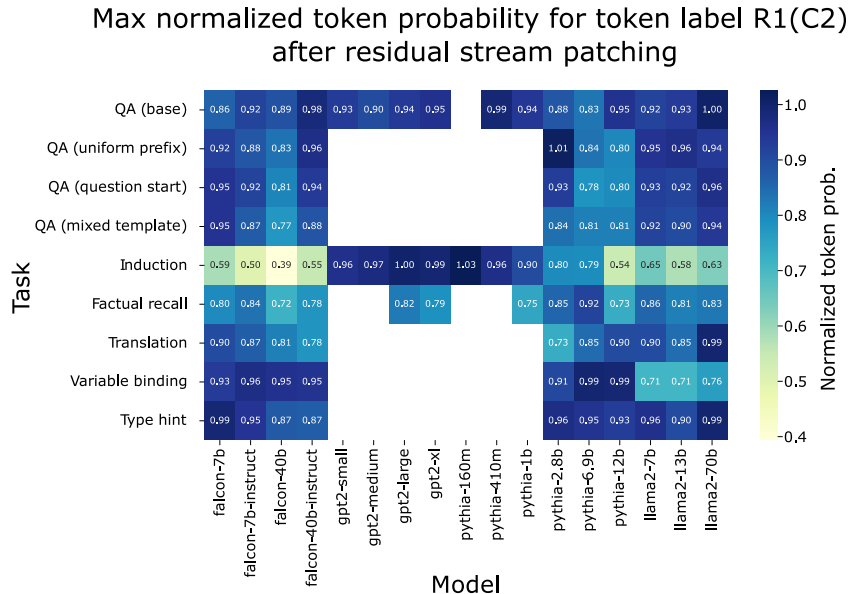


Figure 13: Maximal normalized probability of the $R_1(C_2)$ label token after residual stream patching on all models and tasks from ORION. Request-patching generalizes to the vast majority of tasks and models studied. White regions correspond to settings where the model is unable to robustly solve the task.

- **Multi-token request patching.** Our current method only handles single-token outputs, but real applications require generating multiple tokens. The key technical challenge is maintaining coherent request processing across multiple generation steps. This requires investigating whether the modular separation we observed extends to multi-token generation.

D ADDITIONAL RESIDUAL STREAM RESULTS

Figure 13 shows the maximal normalized probability of the $R_1(C_2)$ label token after residual stream patching. Request patching is robustly working for all model and tasks, except for the induction task. We discuss further the results for induction in Appendix F.

Figure 14 shows side-by-side the results of residual stream patching on the question-answering task. For all models, there exists a span of intermediate layers (40-80% of the model depth) where residual stream patching leads the model to output $R_1(C_2)$ with a high probability (>80% normalized probability). This span of layers seems to be the same for the base and fine-tuned Falcon models. This is coherent with the intuition that fine-tuning is only superficially affecting the model internals.

Figure 15 shows the layers L_1 and L_3 for every model and task studied. We observe a similar motif as in the layer L_2 in Figure 4. The processing for the induction task seems to happen earlier than the other tasks such that all three limit layers are shifted toward the early layers.

However, this trend does not hold for Llama 2 70b. All the limit layers for this model seem to be concentrated over a very narrow span of layers in the middle of the network. To further explore this surprising observation, Figure 16 shows the results of residual stream patching on Llama 2 70b for the factual recall, induction, and translation tasks. The normalized token probability seems to peak in a narrow range of layers (40-43) for all three tasks, including the simple induction task. It is unclear why only Llama 2 70b exhibits this pattern, contrasting with models of similar sizes (e.g. Falcon 40b) that demonstrate spread-out limit layers. This phenomenon could be caused by the larger scale of the model or peculiarities of the architecture.

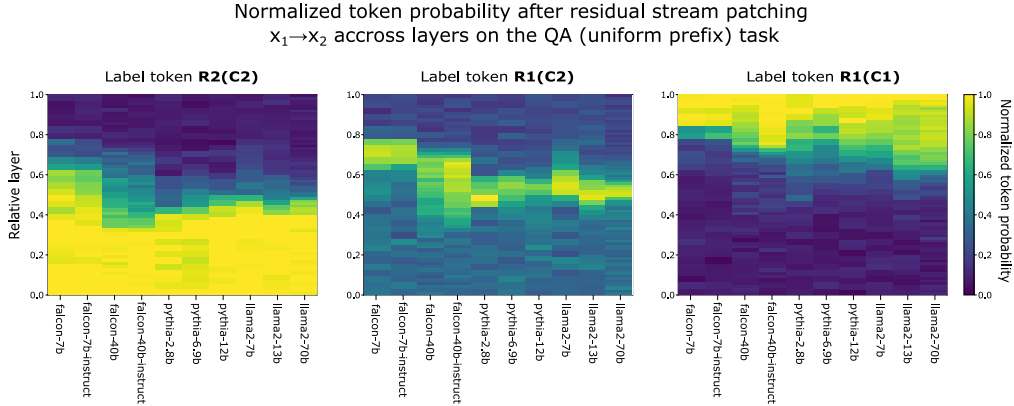


Figure 14: Normalized probability of the label tokens after residual stream patching across all layers on the question-answering task with uniform prefix. To enable comparison across models, we use the relative layer with 0 as the first and 1 as the last layer. Request-patching is general across models: mid-layer residual stream patching causes the model to output $R_1(C_2)$ with more than 80% normalized token probability.

E CAUSAL ABSTRACTION

Validating the high-level causal graph using the framework of causal abstraction. In this Appendix, we express the implications of request-patching on the high-level structure of the computation happening in language models solving retrieval tasks using the framework of causal abstraction (Geiger et al., 2023). We define a high-level causal graph operating on the abstract input representation and an alignment mapping each intermediate variable in the high-level causal graph to a set of model components. The input-output alignment is defined by the ORION abstract input and output representation. The alignment is illustrated in Figure 17.

Our causal graph is a simple two-step symbolic algorithm that treats the request and context separately before combining them to algorithmically solve the retrieval task.

We validate the alignment using interchange intervention accuracy (IIA). IIA is defined in Geiger et al. (2023) as an average over every possible multi-input interchange intervention. However, this average introduces statistical distortion in the case of the alignment we are considering. Because of the shape of our causal graph, interchanging a variable late in the graph screens off the effect of the interchange happening earlier in the graph. Thus, intervening simultaneously on early and late variables is equivalent to interchanging the late variable alone. To remove this statistical distortion, we average the results of the interchange interventions such that each unique experiment gets the same weight.

Moreover, given that residual stream patching is a kind of interchange intervention, we reuse the experimental data from the exploratory causal analysis to compute the IIA. Given the simplicity of our alignment, we can write the IIA for a task T from ORION in terms of three interchange operations as follows:

$$\begin{aligned}
 \text{IIA}_T = \frac{1}{3} E_{x_1, x_2 \in T} & \left[\left[\mathcal{M}(x_2 | z_n^{L_1} \leftarrow z_n^{L_1}(x_1)) = R_1(C_1) \right] \right. \\
 & + \left[\mathcal{M}(x_2 | z_n^{L_2} \leftarrow z_n^{L_2}(x_1)) = R_1(C_2) \right] \\
 & \left. + \left[\mathcal{M}(x_2 | z_n^{L_3} \leftarrow z_n^{L_3}(x_1)) = R_2(C_2) \right] \right]
 \end{aligned}$$

We do not include the results of interchange intervention on the context variable. Given the model architecture, the two interchange operations $\mathcal{M}(x_2 | z_n^L \leftarrow z_n^L(x_1))$ and $\mathcal{M}(x_1 | z_{<n}^L \leftarrow z_{<n}^L(x_2))$

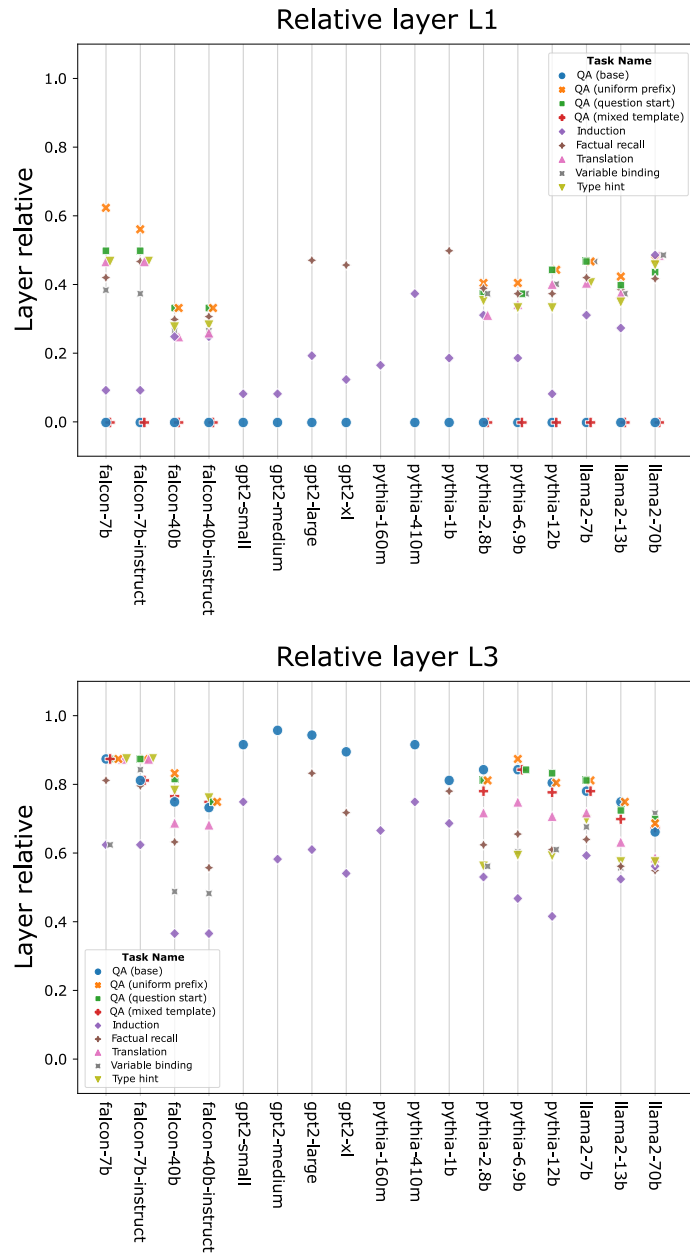


Figure 15: Layer L_1 and L_3 for different models and tasks.

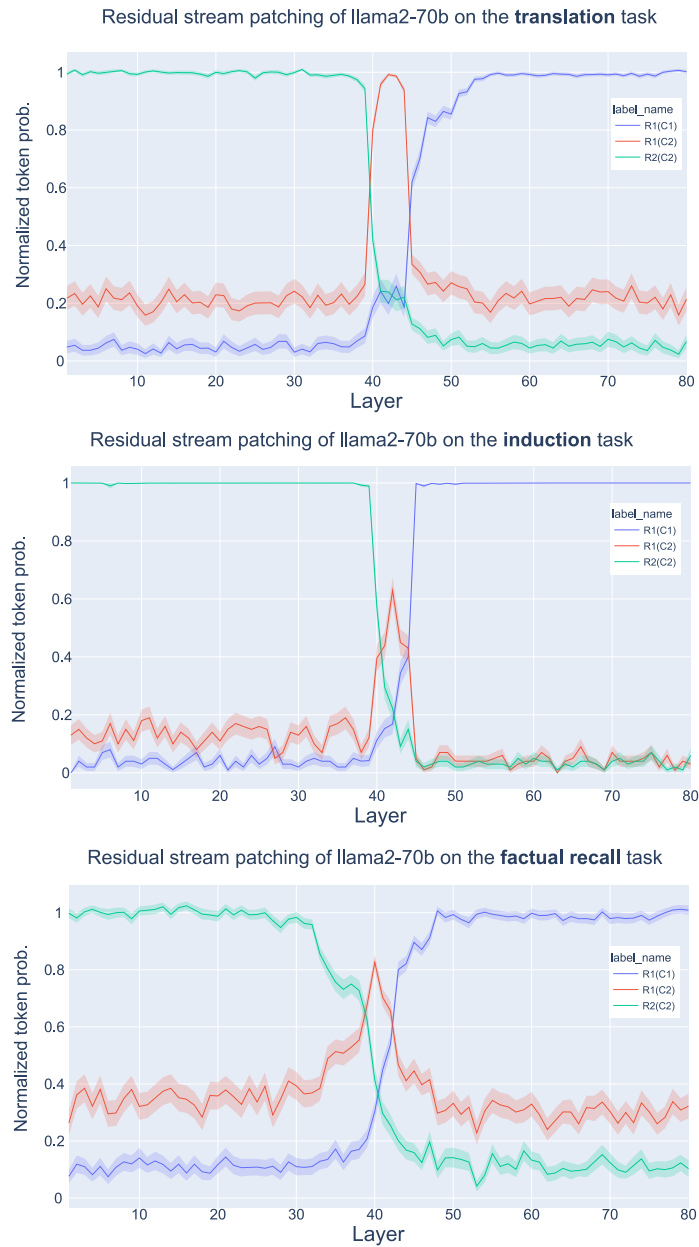


Figure 16: Result of residual stream patching of Llama 2 70b on three retrieval tasks. The maximal effect of residual stream patching, i.e. maximal probability of the label token $R_1(C_2)$, is located at the exact same layer (layer 42) for every task.

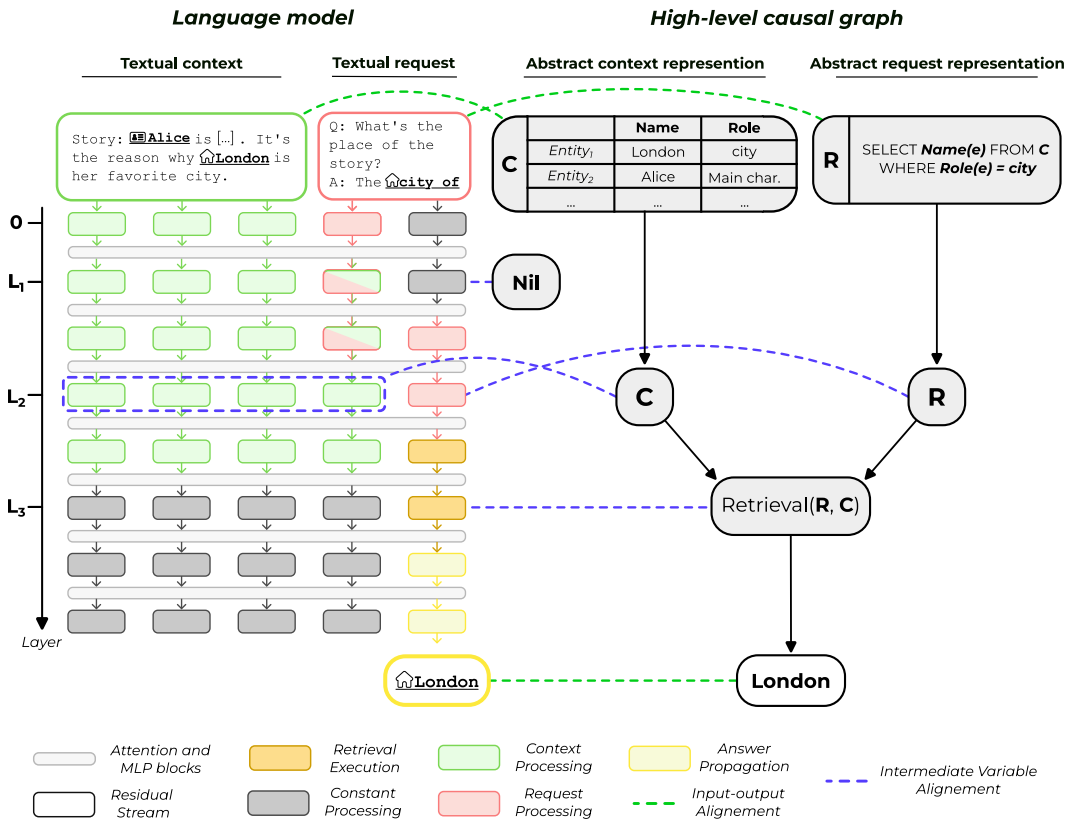


Figure 17: Alignment between a high-level causal graph that uses abstract representations of inputs, and a language model running on the textual representation of the inputs for a retrieval task. The alignment bounds the position where request processing (in red) and context processing (in green) are located in the intermediate layers of the model. The Nil node is isolated in the high-level causal graph. It does not influence the output of the causal graph and thus can be interchanged freely.

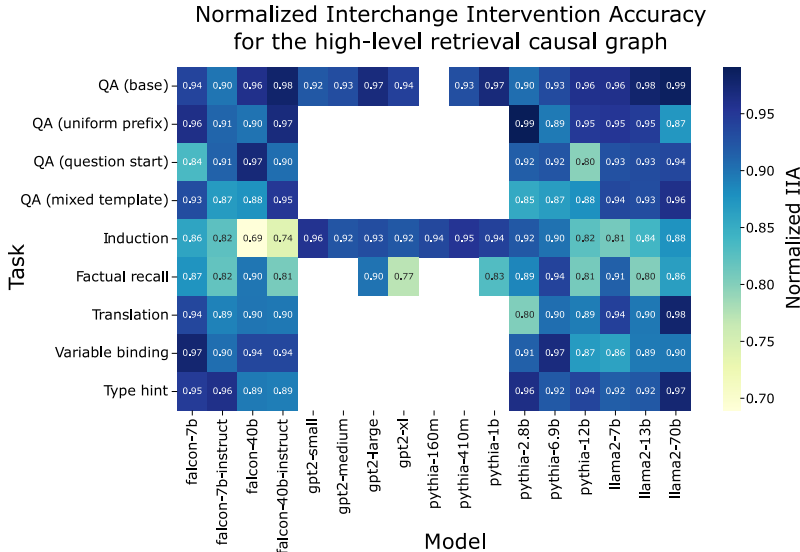


Figure 18: Normalized interchange intervention accuracy for all models and tasks studied for the high-level retrieval symbolic algorithm. The normalized IIA is greater than 85% in 91 out of the 106 settings studied. This demonstrates that our high-level causal graph faithfully describes the internal model computation across different models and tasks.

are equivalent. The first one corresponds to the intervention on the request in the high-level causal graph, and the second corresponds to the intervention on the context. Moreover, our task datasets are defined by independently sampling R and C . This means that by definition, the average output of $\mathcal{M}(x_2|z_n^L \leftarrow z_n^L(x_1))$ and $\mathcal{M}(x_1|z_n^L \leftarrow z_n^L(x_2))$ are the same. We thus remove the results of the intervention on the context from the average to avoid artificial duplication of experimental results.

To facilitate the comparison across tasks, we normalize the IIA such that 0 corresponds to random guesses and 1 is the baseline accuracy on the task. Note that the normalized IIA could be greater than 1 if the causal graph also explains the mistakes of the model. However, we consider a simple high-level causal graph that always answers the correct token such that the baseline model accuracy is a natural upper bound for the IIA.

Finally, it is worth noting that the first and last terms of the expression of IIA_T are dependent on the arbitrary threshold we use to define L_1 and L_3 . Choosing a higher threshold would be an artificial way to increase the IIA. However, this would also make the alignment less expressive as L_1 would tend to be 0, and L_3 would tend to be the last layer, effectively making these parts of the alignment trivial. The thresholds thus represent a tradeoff between the strictness of the hypothesis and the ease of validating it.

The normalized IIA scores for each model and task studied are shown in Figure 18. We observe that the majority of settings studied lead to high IIA scores (91 out of the 106 pairs of models and tasks have scores greater than 85%), showing that the high-level causal model faithfully describes the internal processes of language models on the ORION tasks.

F COMPARISON WITH PRIOR WORK

Factual recall The factual recall and abstract induction tasks from ORION have been previously studied in the mechanistic interpretability literature. In this section, we show that the mechanisms described in previous works are compatible with the results of request-patching.

Previous works studied the factual recall abilities of language models on prompts represented by a triplet (s, r, a) where s is a subject, r is a relation being queried, and a is the corresponding attribute, i.e. the value of the relation on the subject. A prompt would contain the subject and relation while the attribute would define the label token, e.g. “Beat music is owned by” \rightarrow “Apple”. Geva

et al. show that early attention layers at the last token position are used for *relation propagation*, propagating information from the relation token to the last position, e.g. the information about the relation “owned” to the “by” token in the example. Later layers are in charge of *attribute extraction*. They recover the correct attribute from the last subject token, according to the relation propagated to the last position by the earlier layers.

Using the ORION input representation, the relation is part of the request, while the subject is in the context. When performing residual stream patching at intermediate layers, we observe request-patching: the information from the relation in x_1 is transferred but the subject stays the same. Our observation is coherent with the finding from Geva et al. that relation propagation and attribute extraction happen at non-overlapping layers.

Note that contrary to Geva et al. we do not use the dataset Counterfact. This dataset cannot be incorporated into ORION because of the “Decomposable” desiderata for task constellations. Most of the relations in the Counterfact dataset cannot be applied to arbitrary subjects, e.g. a famous person does not have an attribute for the relation “capital city”. To circumvent this limitation, we create two datasets that fit the “Decomposable” desiderata, enabling the design of systematic causal experiments. We document this process in more detail in Appendix H.6.

Induction The induction task consists in completing patterns of the form [A] [B] . . . [A]. For instance, such patterns occur naturally when completing a name that appeared before in the context, e.g. “Harry Potter . . . Harry Pot” \rightarrow “ter”. The mechanisms for induction tasks were first characterized in small two-layer Transformers in (Elhage et al., 2021). The mechanisms involve two steps: the first step consists in previous token heads acting at the [B] position copying the preceding token [A]. The second step involves induction heads acting at the [A] position. In a follow-up paper, Olsson et al. hypothesize that induction heads are also present in large models and recognize more complex patterns with a similar structure such as [A] [B] . . . [A*] (Olsson et al., 2022). In this case, [A] and [A*] can be composed of several tokens and be recognized using fuzzy matching instead of exact token matching. They propose a similar high-level structure as the simple mechanism: the representation at the position [B] is contextualized by incorporating information about the preceding prefix [A], using a more advanced mechanism than the previous token heads. Similarly, the representation of the last token incorporates information about the tokens from [A*]. At later layers, induction heads leverage their attention mechanisms to recognize the similarity between the representations of [A*] at the [B] token position and the representation of [A] at the last token position. Finally, their OV circuit copies the [B] token.

The induction task we designed involves multi-token prefixes with exact matches. We study patterns of the form [A] [X] [B] . . . [A] [X], where [X] is a separator token, a column in our case. According to the extended mechanism for induction, the residual stream at early layers at the last token contains the information propagated from the second [A] occurrence, while the later layer contains induction heads in charge of finding the [B] token in the broader context. If the [A] propagation and the induction heads occur at non-overlapping layers, patching the early residual stream should only modify the representation of the token [A] at the last token position without impacting the retrieval abilities of the induction heads. In the ORION abstract representation, [A] is the request in the induction task. Hence the proposed mechanism for induction heads is coherent with the results of request-patching.

Propagating the [A] token to the final residual stream and the operation of the induction heads are both simple operations, each of these operations can theoretically be performed in a single layer. We hypothesize that these two operations are performed redundantly by two sets of components acting in tandem, a first set to propagate information from [A] to the last token, and a second set of induction heads. We hypothesize that these two sets of components are situated at overlapping layers in large models as part of pre-processing happening in early layers. Large models have the capacity for redundant parallel computation because of their large number of attention heads per layer. This hypothesis would explain the lower performance of request-patching on induction tasks in large models. No layer separates the request and its processing: due to the simplicity of the task, they both happen in parallel.

G TRANSFORMER ARCHITECTURE

In this appendix, we provide a complete description of the Transformer architecture. The pre-softmax values π_n are the logits at the n -th token position. For the GPT-2 Transformer architecture (Radford et al., 2019) with L layers, the function \mathcal{M}_θ can be further broken down as follows:

$$\begin{aligned}\pi_n &= \text{LN}(z_n^L)W_U \\ z_k^l &= z_k^{l-1} + a_k^l + m_k^l \\ m_k^l &= \text{MLP}(z_k^{l-1} + a_k^l) \\ &= \text{LN}(W_{out}(\text{GELU}(W_{in}(z_k^{l-1} + a_k^l) + b_{in})) + b_{out}) \\ a_k^l &= \text{Attn}(z_{\leq k}^{l-1}) \\ z_k^0 &= W_E t + W_P\end{aligned}$$

The final logits π_l are constructed by iteratively building a series of intermediate activations z_k^l we call the *residual stream*, following Elhage et al. (2021). The residual stream z_k^l at token position k and layer l is computed from the residual stream at previous token positions at the previous layer $z_{\leq k}^{l-1}$ by adding the results of Attn, a multi-headed attention module, and MLP, a two-layer perceptron module.

The MLP module depends on the residual stream z_k^{l-1} at position k and layer $l-1$ while the attention module can aggregate information from the previous layer across every previous token position. The residual stream is initialized with the embeddings computed from the token and positional embedding matrices W_E , W_P , and the one-hot encoding of the input tokens t . Finally, W_U is the unembedding matrix, GELU the Gaussian error linear unit activation function (Hendrycks and Gimpel, 2016), and LN is a layer normalization function (Ba et al., 2016) applied to the final residual stream and the output of each module.

In practice, the models we study have slight deviations from the GPT-2 architecture. The Pythia (Biderman et al., 2023), Falcon (Almazrouei et al., 2023) and Llama 2 (Touvron et al., 2023) models use parallelized attention and MLP. In the formulae above, this translates as $m_k^l = \text{MLP}(z_k^{l-1})$. Moreover, Falcon contains additional layer normalization at the input of modules. Llama 2 uses the SwiGLU activation function (Shazeer, 2020) and layer normalization only at the input of modules.

H ORION PROMPTS

Table 5 provides a succinct overview of the task included in ORION.

H.1 DETAILED DESCRIPTION OF THE DATASET DESIDERATAS

1. **Structured.** Every textual input in ORION accepts an abstract representation using the context and request representation defined above. *Motivation: Providing a unified structure to define and interpret causal interventions without the need for setting-specific labor.*
2. **Decomposable.** For every dataset D in ORION, for every abstract representations $(C_1, R_1), (C_2, R_2)$ in D , $R_2(C_1)$ and $R_1(C_2)$ are well-defined. This means that an arbitrary request can be applied to an arbitrary context from the same task. Abstract representations of requests and contexts can be freely interchanged across a task. *Motivation: Enabling the design of interchange interventions.*
3. **Single token.** For every dataset D in ORION, for every abstract representations $(C_1, R_1), (C_2, R_2)$ in D , $R_1 = R_2 \Leftrightarrow R_1(C_1) = R_2(C_1)$. In other words, in a given context, the output of each request gives a unique answer. It ensures that measuring the next-token prediction is enough to know which request has been answered. *Motivation: Making experiments easy to measure and computationally efficient.*
4. **Monotasking.** For every dataset D in ORION, for every abstract representation (C, R) in D , there is a unique line in C such that $\text{ATTR}_f = v_f$. This condition ensures that requests

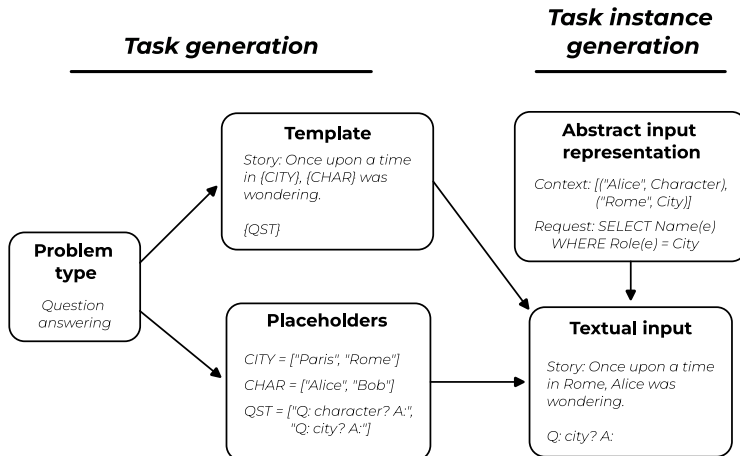


Figure 19: The semi-automatic task generation process used to create ORION. We use ChatGPT to create a template and values for the placeholders given a problem type. To generate an instance from the task, we start by randomly selecting placeholder values to create an abstract input representation. Then, we use a format string to fill the template. When we need more flexibility, we use GPT-4 to incorporate the placeholder values into the template.

are answerable with unambiguous answers. *Motivation: Making analysis tractable. It is easier to understand models solving a single problem than solving multiple problems in parallel.*

5. **Flexible.** ORION contains diverse tasks spanning multiple domains and levels of complexity. In practice, we demonstrate the flexibility of the ORION structure by creating 15 different tasks spanning six different language model abilities. *Motivation: Enabling rich comparative analysis across models and domains.*

In the code implementation, we designed automatic tests to ensure that conditions “Decomposable”, “Single token”, and “Monotasking” are respected for every task in ORION.

H.2 DATASET CREATION

To create the ORION task datasets, we use a semi-automatic process illustrated in Figure 19, leveraging the creative writing ability of ChatGPT². Concretely, we use the following workflow:

1. Find a problem that can be formulated as a retrieval task, e.g. question-answering.
2. Use ChatGPT to create a template with placeholders, e.g. a story with placeholders for narrative variables such as the city, the name of the character, and the question being asked.
3. Use ChatGPT to create a set of placeholders.
4. Procedurally generate a set of abstract representations for the contexts and requests.
5. Generate the textual inputs from the abstract representation using format strings or ChatGPT when more flexibility is required.

We applied this workflow to create 15 tasks spanning six problem domains requiring different abilities: question answering, translation, factual recall, variable binding, abstract pattern matching (induction pattern) and coding. For each domain, we created variation of surface-level parameters of the task (e.g. changing language of the translation). We give an example input-output pair for each in Table 5. We provide a detailed discussion about task choices as well as a precise description of each dataset in the rest of this Appendix.

²<https://chat.openai.com/>

Task name	Example Prompt	Label token	Variations
Question-answering (base)	<p>Story: In the lively city of Valencia, spring mornings [...] as a skilled veterinarian [...] "I'm Christopher" he replied, [...].</p> <p>Question: What is the name of the main character? Answer: The main character is named</p>	Christopher	1
Question-answering (uniform prefix)	<p>Story: In the lively city of Valencia, spring mornings [...] as a skilled veterinarian [...] "I'm Christopher" he replied, [...].</p> <p>Question: What is the name of the main character? Answer: The answer is "</p>	Christopher	1
Question-answering (question first)	<p>Question: What is the name of the main character?</p> <p>Story: In the lively city of Valencia, spring mornings [...] as a skilled veterinarian [...] "I'm Christopher" he replied, [...].</p> <p>Answer: The answer is "</p>	Christopher	1
Question-answering (mixed templates)	Uniform distribution of prompts from three variations of question-answering above.		1
Translation	<p>English: In an era defined by increasing global temperatures [...] At the forefront is M. Smith, a marine biologist [...] Next, we turn to M. Miller, a climate economist [...]</p> <p>French: [...] Nous nous tournons ensuite vers M.</p>	Miller	3
Factual recall	<p>Question: On which continent did Muhammad Ali live? Answer:</p>	America	2
Variable binding	<p>Anthony has a collection of pencils. 50 pencils are blue, 10 pencils are red, and 20 pencils are green.</p> <p>How many pencils in total are either blue or green? We'll add the number of green pencils (</p>)	3
Induction pattern-matching	<pre>xnGWu:nJIbF etmNX:TzgIS ZvcIf:Gcqvs [...] AjvIA:pXMgi etmNX:</pre>	T	1
Type hint understanding	<pre>def calculate_circumference(circle: Circle) -> float [...] W = Rectangle(Point(2, 3), Point(6, 5)) D = Circle(Point(0, 0), 5) print(calculate_circumference(</pre>	D	3

Table 5: Tasks from the ORION collection contain varied problem type and prompt format. For readability, we use “[...]” to shorten the prompts. The rest of the text is part of the textual input. In particular, “[...]” is part of the prompt for the translation task. We use “_” to indicate a space in the label token.

H.3 DISCUSSION ABOUT TASK CHOICE

For a given problem type, we generate several templates, enabling the creation of several task variations. We use this procedure to generate 15 unique tasks spanning six different abilities.

We use several criteria in choosing the problem types. First, we choose tasks that have already been studied in the literature to act as reference points for our analysis. This includes factual recall and the induction task. Then, to allow analysis across model scales, we design a simple question-answering task that can be solved by both small and large models. We also create more challenging tasks to explore diverse skills such as coding abilities, tracking the association between an object and its quantity, and tasks involving translation from English to three different languages.

In addition to diversifying the content of the tasks, we create structural modifications to the task template. To that end, we create question-answering templates where the question is before the story in the dataset and templates where the final token of the prompt does not depend on the request. We also create a mixed question-answering task containing prompts from the three variations.³

In this rest of this Appendix, we describe in more detail the process we used to create each task of the ORION collection. We also provide complete example prompts for each task.

H.4 QUESTION-ANSWERING

H.4.1 GENERATING THE STORIES

We created a set of 100 stories we used in the four variations of the question-answering task. Each story was created by defining:

- The name of the main character
- The occupation of the main character
- The time of day
- The season of the year
- The city of the story
- The action of the story
- An order in which the above elements should be introduced in the story
- An example story called a “master story”, used as a template to incorporate the new narrative elements

The value of each of the narrative elements was uniformly sampled from lists of 3 to 5 different possible values for each field. The lists were generated using manual interaction with ChatGPT.

The 8 narrative elements were combined in a prompt shown in 20 and completed by GPT-4. The goal of this process was to reduce as much as possible the variations introduced by GPT-4, such that the variables in the generation prompt characterized the generated story as comprehensively as possible.

H.4.2 GENERATING THE QUESTIONS

We manually generated questions and answer prefixes about three different narrative variables: character occupation, city, and name of the main character. For each narrative variable, we created three different phrasings.

The answer prefixes were either uniform, as shown in Figures 21 and 22 for the task variation with uniform prefix and question at the start, or depended on the variable queried in the question, as shown in Figure 23 for the base task variation. The base task variation can be solved by smaller models, while only larger models can handle uniform answer prefixes.

³Given that the mixed-template task is an aggregation of other task variations, we do not include it in the count of 15 unique tasks.

```

You have to generate a short story that fits in a single paragraph
of less than 150 words. It has to respect a list of precise
constraints.

### Narrative elements

The main character is named {character_name}. Their occupation is
{character_occupation}. The story takes place in {city}. The time
of the day is the {day_time}, and the season is {season}. The time
of the day should stay constant in the story. The action
performed by the main character is {action}.

It's crucial that all the elements appear in the story.

### Order of the narrative elements

The order in which to introduce the narrative elements is imposed.
The main priority is to respect the order of apparition I impose.
Here is the imposed order in which to introduce the narrative
elements. This order is already present in the template story.

{variable_order}

### Template story

You have to generate a story that matches as closely as possible a
template story. Your goal is to modify the template story such
that all the narrative elements are present, but the general
structure (e.g. order in which the narrative element are
introduced etc.) is as close as possible to the template story.

Here is the template story you have to stick to:

"{master_story_text}"

Generate a short story that matches the template story while
incorporating the new narrative elements.

```

Figure 20: Prompt used to generate the stories for the question-answering tasks. The variables in curly brackets represent placeholders that were replaced by values randomly sampled from manually created lists of possible values.

H.5 TYPE HINT UNDERSTANDING

Using ChatGPT, we generated three Python code snippets introducing new classes and functions using these classes, as shown in Figure 24. The context is a set of variables with a given type. The request asks for a variable name with a particular type. The function definitions do not vary across prompts and are only used to formulate the request.

H.6 FACTUAL RECALL

Existing open-source datasets created to study factual recall in language models, such as the one introduced in (Meng et al., 2022), contain relations (e.g. the sport of an athlete) that can only be applied to a subset of the subjects (e.g. only athletes, since asking the sport played by a country does not make sense). This makes it impossible to use causal intervention such as the type required for request-patching (the desiderata “Decomposable” is not fulfilled). Thus, we created two variations of factual recall tasks such that any pair of subject and relation exists. Contrary to the other task from ORION, the retrieval tasks do not involve copying an attribute present in the context, the task requires the model to know the attribute.

Context

```
<|endoftext|>
```

Here is a short story. Read it carefully and answer the questions below with a keyword from the text. Here is the format of the answer: 'The answer is "xxx".'

The morning sun bathed the streets of Cusco in a warm, golden light, casting long shadows that danced along with the gentle summer breeze. Amidst the bustling city, a tall, slender figure stood on the rooftop of an unfinished building, their eyes surveying the urban landscape below. As the skyline slowly transformed under their careful guidance, it became apparent that the person was no mere observer, but an architect, orchestrating the symphony of steel and concrete. The sound of birdsong filled the air, but it was soon joined by another melody -- the architect's voice, soaring with joy and passion, a song of creation and ambition. And as the last notes faded away, the wind carried a whispered name, the signature of the artist who painted the city with their dreams: Michael.

Answer the questions below.

Request

Question: What job does the main character have?

Answer: The answer is "

Figure 21: Example prompt for the QA (uniform prefix) task.

Geography dataset We used an open-source database⁴ of countries. We extracted the name, capital city, and continent of each country.

Geography dataset Following the process used in (Krasheninnikov et al., 2023), we used a Cross-Verified database (CVDB) of notable people 3500BC-2018AD (Laouenan et al., 2022). Each individual was ranked by popularity (measured with the “wiki_readers_2015_2018 feature“), and 4000 of the most popular individuals were taken (2000 men and women each). We selected the fields related to the gender, continent, and nationality of each notable person.

Filtering For both datasets, we queried the relation about the entity using a few shot setting, as shown in Figure 25. From the raw data extracted from the dataset, we further filtered the list of entities to keep only the ones where GPT-2 was able to answer all the questions related to the entity. The final dataset contains 243 notable people (i.e. 729 questions) and 94 countries (i.e. 282 questions).

H.7 VARIABLE BINDING

We were inspired by the shape of grade school math problems from the GSM8K dataset (Cobbe et al., 2021). The goal was to create retrieval tasks that would naturally occur in a chain of thought generated by a model solving a math puzzle. The context contains objects with different quantities. The request asks for the quantity of an object type.

To create the dataset, we picked one sample from the GSM8K dataset and generated variations using ChatGPT. An example prompt can be found in Figure 26.

⁴<https://github.com/annexare/Countries>

Request

```
<|endoftext|>
```

Read the question below, then answer it after reading the story using a keyword from the text. Here is the format of the answer: 'The answer is "xxx".'

Question: What job does the main character have?

Context

Story: The morning sun bathed the streets of Cusco in a warm, golden light, casting long shadows that danced along with the gentle summer breeze. Amidst the bustling city, a tall, slender figure stood on the rooftop of an unfinished building, their eyes surveying the urban landscape below. As the skyline slowly transformed under their careful guidance, it became apparent that the person was no mere observer, but an architect, orchestrating the symphony of steel and concrete. The sound of birdsong filled the air, but it was soon joined by another melody -- the architect's voice, soaring with joy and passion, a song of creation and ambition. And as the last notes faded away, the wind carried a whispered name, the signature of the artist who painted the city with their dreams: Michael.

Answer: The answer is "

Figure 22: Example prompt for the QA (question first) task.

H.8 TRANSLATION

We used ChatGPT-3.5 (referred to as ChatGPT in the main text and the rest of the Appendix) to generate news articles using placeholders instead of real names. We instructed it to add as many names as possible and to prefix each name with a common title, such as "M.". Then, we asked ChatGPT to translate the text into a non-English language. From the translated text we extracted excerpts that preceded each of the names but did not include any names. These excerpts formed the request. When creating the dataset, the placeholders are replaced by distinct family names from a list generated by ChatGPT.

Using this process, we created three variations with different subjects, target languages, and name prefixes.

- Title: "Climate Change: The Unsung Heroes", Prefix: "M.", Target language: French.
- Title: "Hidden Wonders Revealed: New Species Discovered in Unexplored Amazon Rainforest", Prefix: "Dr.", Target language: Spanish.
- Title: "From Pirates to Naval Heroes: Captains who Shaped Maritime History", Prefix: "Capt.", Target language: German.

The entities in the context are the named characters, and their attribute is the sentence in which they appear. The request is asking for a name that appears in a given sentence.

H.9 INDUCTION

We generated 10 pairs of random strings made from upper and lower-case letters separated by a column. The context contains five enumerations of the pairs. Each enumeration is in a random order. The request is the first half of one of the pairs. An example prompt is shown in Figure 28.

Context

<|endoftext|>

Here is a short story. Read it carefully and answer the questions below.

The morning sun bathed the streets of Cusco in a warm, golden light, casting long shadows that danced along with the gentle summer breeze. Amidst the bustling city, a tall, slender figure stood on the rooftop of an unfinished building, their eyes surveying the urban landscape below. As the skyline slowly transformed under their careful guidance, it became apparent that the person was no mere observer, but an architect, orchestrating the symphony of steel and concrete. The sound of birdsong filled the air, but it was soon joined by another melody -- the architect's voice, soaring with joy and passion, a song of creation and ambition. And as the last notes faded away, the wind carried a whispered name, the signature of the artist who painted the city with their dreams: Michael.

Answer the questions below, The answers should be concise and to the point.

Request

Question: What job does the main character have?

Answer: The main character is a professional

Figure 23: Example prompt for the QA (base) task.

Context

```

<|endoftext|>
from typing import List
from math import pi

class Point:
    def __init__(self, x: float, y: float) -> None:
        self.x = x
        self.y = y

class Rectangle:
    def __init__(self, bottom_left: Point, top_right: Point) -> None:
        self.bottom_left = bottom_left
        self.top_right = top_right

class Circle:
    def __init__(self, center: Point, radius: float) -> None:
        self.center = center
        self.radius = radius

class Polygon:
    def __init__(self, points: List[Point]) -> None:
        self.points = points

def calculate_area(rectangle: Rectangle) -> float:
    height = rectangle.top_right.y - rectangle.bottom_left.y
    width = rectangle.top_right.x - rectangle.bottom_left.x
    return height * width

def calculate_center(rectangle: Rectangle) -> Point:
    center_x = (rectangle.bottom_left.x + rectangle.top_right.x) / 2
    center_y = (rectangle.bottom_left.y + rectangle.top_right.y) / 2
    return Point(center_x, center_y)

def calculate_distance(point1: Point, point2: Point) -> float:
    return ((point2.x - point1.x) ** 2 + (point2.y - point1.y) ** 2) ** 0.5

def calculate_circumference(circle: Circle) -> float:
    return 2 * pi * circle.radius

def calculate_circle_area(circle: Circle) -> float:
    return pi * (circle.radius ** 2)

def calculate_perimeter(polygon: Polygon) -> float:
    perimeter = 0
    points = polygon.points + [polygon.points[0]] # Add the first point at the end for a closed shape
    for i in range(len(points) - 1):
        perimeter += calculate_distance(points[i], points[i + 1])
    return perimeter

# Create a polygon
Y = Polygon([Point(0, 0), Point(1, 0), Point(0, 1)])

# Create a rectangle
K = Rectangle(Point(2, 3), Point(6, 5))

# Create a circle
P = Circle(Point(0, 0), 5)

```

Request

```

# Calculate area
print(calculate_area(

```

Figure 24: Example prompt for the type hint understanding task.

CVDB prompt

```
<|endoftext|>Question: What was the country of Freddie Mercury?  
Answer: UK  
  
Question: On which continent did Muhammad Ali live?  
Answer: America  
  
Question: What was the country of Fela Kuti?  
Answer:
```

Geography prompt

```
<|endoftext|>Question: What is the capital of France?  
Answer: Paris  
  
Question: What is the language spoken in Malaysia?  
Answer:
```

Figure 25: Example prompt for the factual recall task on the CVDB and geography datasets. There is no clear division between context and request in the prompt. In full rigor, the context is composed of a single entity, e.g. 'Fela Kuti' in the first prompt, while the request is asking about an attribute, e.g. the country, without filtering as there is a single entity in the context.

Context

```
<|endoftext|>John is baking cookies. The recipe calls for 4 cups  
of flour, 2 cups of sugar, and 6 cups of chocolate chips. How many  
cups of ingredients in total are needed for the cookies?
```

Request

```
We'll add the number of cups of flour (
```

Figure 26: Example prompt for the variable binding task.

Context

```
<|endoftext|>
Here is a new article in English. Below, you can find a partial translation in French
. Please complete the translation.

English:

Title: "Climate Change: The Unsung Heroes"

In an era defined by increasing global temperatures and extreme weather events, the
fight against climate change continues on many fronts. While prominent
environmentalists and politicians often claim the limelight, behind the scenes,
countless unsung heroes have dedicated their lives to combating climate change. This
article aims to spotlight the work of these individuals.

At the forefront is M. Jones, a marine biologist who has developed an innovative
method for promoting coral reef growth. Given that coral reefs act as carbon sinks,
absorbing and storing CO2 from the atmosphere, M. Jones's work has significant
implications for climate mitigation. Despite facing numerous hurdles, M. Jones has
consistently pushed forward, driven by an unwavering commitment to oceanic health.

Next, we turn to M. Martinez, a climate economist from a small town who has
successfully devised a market-based solution to curb industrial carbon emissions. By
developing a novel carbon pricing model, M. Martinez has enabled a tangible shift
toward greener industrial practices. The model has been adopted in several countries,
resulting in significant reductions in CO2 emissions. Yet, despite these successes,
M. Martinez's work often flies under the mainstream media radar.

Another unsung hero in the climate change battle is M. Perez, a young agricultural
scientist pioneering a line of genetically modified crops that can thrive in drought
conditions. With changing rainfall patterns threatening food security worldwide, M.
Perez's work is of immense global relevance. However, due to controversy surrounding
genetically modified organisms, the contributions of scientists like M. Perez often
go unnoticed.

Additionally, the story of M. Thomas is worth mentioning. An urban planner by
profession, M. Thomas has been instrumental in designing green cities with a minimal
carbon footprint. By integrating renewable energy sources, promoting public
transportation, and creating more green spaces, M. Thomas has redefined urban living.
While the aesthetics of these cities often capture public attention, the visionary
behind them, M. Thomas, remains relatively unknown.

Lastly, we have M. Harris, a grassroots activist working tirelessly to protect and
restore the forests in her community. M. Harris has mobilized local communities to
halt deforestation and engage in extensive tree-planting initiatives. While large-
scale afforestation projects often get global recognition, the efforts of community-
level heroes like M. Harris remain largely unsung.

The fight against climate change is not a single battle, but a war waged on multiple
fronts. Every victory counts, no matter how small. So, as we continue this struggle,
let's not forget to appreciate and honor the unsung heroes like M. Jones, M. Martinez
, M. Perez, M. Thomas, and M. Harris who, away from the spotlight, are making a world
of difference.
```

Request

```
French:
[...]
En intégrant des sources d'énergie renouvelables, en favorisant les transports
publics et en créant plus d'espaces verts, M.
```

Figure 27: Example prompt for the translation task.

Context

```
<|endoftext |>wFCJI:CCwti
axRPX:ISNak
JaVZO:jjVAE
vGuLv:aqCuW
peaXt:uqIWZ
gLbzR:URzLs
XPUGR:QDKMS
IbKIs:YRodj
GpqLd:YRodj
fhVqk:jjVAE
axRPX:ISNak
gLbzR:URzLs
wFCJI:CCwti
GpqLd:YRodj
fhVqk:jjVAE
vGuLv:aqCuW
XPUGR:QDKMS
peaXt:uqIWZ
IbKIs:YRodj
JaVZO:jjVAE
axRPX:ISNak
XPUGR:QDKMS
wFCJI:CCwti
IbKIs:YRodj
gLbzR:URzLs
peaXt:uqIWZ
vGuLv:aqCuW
JaVZO:jjVAE
GpqLd:YRodj
fhVqk:jjVAE
wFCJI:CCwti
GpqLd:YRodj
peaXt:uqIWZ
gLbzR:URzLs
XPUGR:QDKMS
axRPX:ISNak
JaVZO:jjVAE
IbKIs:YRodj
fhVqk:jjVAE
vGuLv:aqCuW
peaXt:uqIWZ
XPUGR:QDKMS
wFCJI:CCwti
JaVZO:jjVAE
IbKIs:YRodj
fhVqk:jjVAE
gLbzR:URzLs
axRPX:ISNak
GpqLd:YRodj
vGuLv:aqCuW
peaXt:uqIWZ
gLbzR:URzLs
GpqLd:YRodj
peaXt:uqIWZ
GpqLd:YRodj
fhVqk:jjVAE
GpqLd:YRodj
XPUGR:QDKMS
peaXt:uqIWZ
```

Request

```
wFCJI:
```

Figure 28: Example prompt for the induction task.